C O V E N T R Y
U N I V E R S I T Y

Faculty of Engineering, Environment and Computing

School of Computing Electronics and Mathematics

Path Planning and trajectory tracking of a miniature 1D capsule robot for medical applications.

Author: Abas Mohammedidris (8931834)
Supervisor: Dr John Arvanitakis

Submitted in partial fulfilment of the requirements for the Degree of Bachelor of Electrical and Electronic Engineering

Academic Year: 2019/20

Declaration of Originality

I hereby declare that, this thesis is my own work except where specific reference is made acknowledging others work.

Copyright

I would like to dedicate this thesis to my family without them I wouldn't be able to become who I am today.

Acknowledgment

I would like to use this page to honour all my mentors, family and friends who supported me through this journey.

I would like to express my sincere gratitude to my supervisor Dr John Arvanitakis who always inspired me and provided me with invaluable support for completion of this work, specially throughout this tough time of lockdown.

I would like also to thank my previous supervisor Dr Nazmul Huda for giving me the opportunity to work on this project and for all the information and materials he provided me with for this project.

I would like to express my gratitude to all my teachers throughout my education years, those who taught me everything and gave the knowledge to get where I am today, without their support, encouragement and guidance all this would not be possible.

I would like to thank all my friends for their unlimited support, specially my dearest friends Dawood and Sami.

Greatest thanks go to his almighty Allah and his Rusul for providing me with the strength, patience and everything I have today.

Abstract

Recently, the research on capsule robots(capsubot) has attracted extensive attention by researchers, this class of robots are limbless, which means, the external structure of the robot is flexible and due to this flexibility the capsubot can be used in medical applications, engineering diagnosis such as pipe inspection and disaster rescue.

Driven by the requirement, this thesis presents and investigates different topics of 1D capsule robot (capsubot) which is a class of underactuated mechanical system. This thesis mainly focus is, on mathematical modelling of the capsubot with different friction models and investigating the performance of the system with a basic and advanced friction model.

Choosing the right friction models for dynamic modelling is very important, friction model that captures most of the friction regime in various circumstances such as in low velocity, high velocity and zero velocity is the main aim of this research. In terms of motion generation, four possible scenarios are used with two acceleration profiles. Due to the capsubot mechanical property which is underactuated and the degree of freedom to be controlled is higher than the control input, therefor a two-stage controller is used. The first stage is creating desired trajectory for the inner mass and the capsubot using a selection algorithm. The second stage is for the given desired trajectory, the close-loop control is achieved by correcting the input using the error.

The capsubot system dynamic is non-linear, because the differential equation governing the system is non-linear, however most of the theories have been developed based on linear system, therefore this thesis proposes a method on how to linearize the capsubot system.

Key words: capsubot, dynamic modelling, friction models, motion generation, control of (UMS), state-space representation, linearization of non-linear system.

Table of Contents

List of figures

List of tables

Chapter one

1.1 Introduction and background

In recent years many researches have been attracted on researching on capsule robots (capsubot) and conducted intensive research on various aspect of it, such as mathematical modelling, control, trajectory tracking etc. This class of robots have gained attention because of its wide application in engineering diagnosis, disaster rescue and medical application. The (capsubot) is a limbless which makes it's external structure flexible. On this design the capsubot can only move on one direction because it is on dimension and this class of robots motion has been studied on (Li et al. 2006), (Yu et al. 2008), (Liu et al. 2008), (Huda et al. 2011) and which operates on the principle of internal force and dry friction to create motion and the principle is derived in (Yamagata and Higuchi 1995).

The existing designs of mobile robots for capsule endoscope for gestor-intestinal can be categorised based on the locomotion mechanism as external propulsion robot (Mahoney and Abbott 2014), (Rahman et al. 2015) , internal propulsion robot (Platt et al. 2009), (De Falco et al. 2014), (Yu et al. 2011) and hybrid propulsion robot (Simi et al. 2010).However , this thesis will be focused on the internal propulsion robot . the advantages of the internal propulsion robots are, can accomplish a control of position with higher precision because they consist of actuators onboard .However this could be disadvantage because internal propulsion robots require actuators and to drive the actuators a power source is required e.g. battery and this could be challenging to accommodate within the main the body of the robot.

Mathematical modelling of underactuated mechanical system , the robot under consideration on this thesis is 1-dimentional capsule robot (capsubot) which is class of underactuated mechanical system , such system can be modelled in various ways such as using newton's second law of motion and Euler-Lagrange ,however choosing the friction model to capture the friction regime is very important .

the friction phenomena is the reaction direction between surfaces whose are in contact and modelling the friction phenomena have been an active area of research since the coulombs hypothesis (coulomb 1785) and the friction regime can be treated as results of different factors such as the contact surfaces material properties ,its shape ,relative velocity and displacement of the pair in contact.

In systems dynamic modelling , we see that most systems are non-linear , which means the differential equation governing the system's evolution is non-linear , an example of such systems is the capsubot the system under consideration on this thesis .However ,most theories that have been developed are based on linear systems. In order to view the non-linear model of the capsubot as a linear model we need to develop what we call the Jacobean linearization around equilibrium.

1.2 Project Aims Objectives

The aim of this project is to develop a path planning and trajectory tracking of 1D capsule robot (capsubot) for medical applications. Capsubot is limbless robot that has no external moving parts and moves using internal reaction force (Yu et all.2008). The main aim of the project is to model and analyse the capsubot system with different friction models.

- To model the capsubot system mathematically with different friction models.
- To generate motion.
- To control the system so it will follow a desired trajectory.
- To simulate and investigate the performance of the capsubot system with different friction models.
- To linearize the system using linearization method such as Jacobean linearization.

1.3 Thesis outline

Chapter two: this chapter presents a literature review on control of underactuated mechanical system, friction phenomena, dynamic modelling and stat-space representation, needs and challenges of medical application robotics.

Chapter three: this chapter presents dynamic modelling of the system with different friction models, state-space representation of the system, acceleration profiles and motion generation, parameters selection of acceleration profiles and linearization.

Chapter four: this chapter presents the database creation, inner mass and capsubot desired trajectory generation, selection algorithms and inner mass control.

Chapter five: this chapter presents the simulation results for both models and comparison discussion of the results.

Chapter six: this chapter concludes the project and presents achievement that have been made and future work that can be done.

1.4 Methodology

The methods to accomplish this projects aim are shown below

- Conduct intensive background research using keywords: capsubot, underactuated mechanical system, dynamic modelling of underactuated mechanical system, trajectory tracking of capsubot , control of underactuated mechanical system , linearizing non-smooth system and friction phenomena.
- Dynamic modelling of the systems with different friction models.
- Motion generation using the four possible scenarios.
- Controlling the system using the two-stage control strategy method.
- Linearizing the non-linear model by changing the sgn and absolute function by an equivalent approximated function.
- Simulate the system in MATLAB/Simulink and compare performance.

Chapter Two

1.5 Literature Review/Theory

1.5.1 Trajectory tracking and control perspective for under actuated mechanical system

Robotics engineers know the significance of controlling the trajectory tracking in the process design of robotics and so as to achieve that ,numerous difficulties are looked because of dynamic of the systems, the system viable on this thesis is a 1D capsule robot (capsubot), which is an underactuated mechanical system (UMS), the trajectory tracking control of (UMS) it has been one of the difficult issues (Huda and Yu, 2015) ,in all cases the capsubot has one control input created by the piezoelectric component and two variables must be controlled (Liu, Yu and Yang, 2008).

A seven stage motion procedure was proposed and explored utilizing two trajectory control approach open-loop ,close-loop and a third methodology which is a straightforward switch for controlling the capsubot(Liu, Yu and Yang, 2008), the (OLC) utilizes quick and moderate motion stages and for the (CLC) ,the control law was chosen using the feedback linearization as (u $=\alpha\tau_d + \beta$). The (SSC) is not a trajectory tracking based technique yet it can move the capsubot an ideal way, the simulation results for all methodologies inferred that, the (CLC) gives the best performance among the entirety of the proposed trajectory tracking control approaches and it additionally permits the velocity to be tracked however the test with this methodology is hard to implement, the study likewise found that, the (OLC) gives good performance for one cycle and this could be because of absence of feedback.

Different strategy for motion generation was proposed by (Lee et al. (2008), which is the four step motion generation approach, in this study the friction coefficient between the internal mass and the surface is assumed extremely small and to make the capsubot move ,the motion is divided into four stages as following the initial step is fast backward with accelerated motion of m_2 ($\ddot{x}_2$<<0)and forward accelerated motion m_1 ($\ddot{x}_1$>0) , the second step is the slow backward deceleration of m_2 ($\ddot{x}_2$>0)and forward deceleration of m_1($\ddot{x}_1$<0) , the third step is slow backward with decelerated motion of m_2 ($\ddot{x}_2$>0) and m_1($\ddot{x}_1 = 0$) remains stationary and the last step is the slow forward motion of m_2($\ddot{x}_1 \leq \epsilon$) and m_1 ($\ddot{x}_1 = 0$) continues to remain stationary.

It was additionally proposed by (Huda and Yu, 2015) two acceleration profiles and two-phase control strategy for motion generation for underactuated mechanical system robot (capsubot) and they are utorque profile and the contraruim profile The utorque profile is a four step acceleration profile, in the initial two steps the capsubot and the inner mass move a similar direction and in the opposite for the last two steps, the IM moves forward which is the (onward journey) for the initial

two steps and in reverse which is the (return journey).The capsubot moves forward in step 1,2,4 and stationary at the initial step 1 as the friction between the capsubot and the surface of motion is higher than the force received by the capsubot. The second acceleration profile is the contraruim profile, which is a two-step acceleration profile, in this profile the capsubot moves in opposite direction of the inner mass (IM), the words utorque and contrarium originate from the Latin words meaning utorque (both directions) and contrarium (opposite direction).
The accompanying two profiles are utilized to track the capsubot, the utorque is used primarily and the contraruim when the velocity changes polarity. This study proposed a novel methodology to control the capsubot however a fully close-loop system experimentation was not conducted.

The capsubot can be modified by including spring since spring can store kinetic energy of the inner mass and return it in the best possible time when it is required, a robot without spring cannot budge if the deriving force is less than friction (Ivanov, 2019), this investigation shows that the error can be corrected by spring swinging the internal mass into resonance and combined the advantage of including of spring with simplicity of formalization.
Different technique which is a feedback linearization for a class of multiple-input and output was presented by (Tuan and Lee, 2016), the study shows, that by applying algebra foundation for investigation in which mathematical model is simplified into matrix equation and by separating the underactuated system into two subsystems actuated and unactuated states and system is designed, so partly applying the non-linear feedback to the two states, however, the stability of unactuated states can't be guaranteed by this controller except if its structure is adjusted to offer steadiness to the two states.
geometric investigation based trajectory tracking and control for class of underactauated capsule system with viscoelastic property was proposed by (Liu et al. 2017), considering the non-collocated dynamic constrains into the control indexes and it was discovered that the viscoelastic interaction plays an active and important role in optimal control .Further investigation was conducted by (Liu et al. 2018) for the issue of adaptive trajectory tracking of vibro-driven capsule robot and a practical motion generation was derived by investigating the dynamic constrains and kernel control indexes and two tracking control were designed using close-loop feedback linearization and an adaptive variable control with auxiliary variable. The investigation brought a novel issue into thought which is the environment factor, where the robot will be used and this was assessed using an adaptive tracking control with the consideration of uncertainty, by assuming the robot mass and friction coefficient uncertain with known limits and this technique was able to ensure the exact tracking of collocated subsystem in simulation based results.

An optimal control strategy dependent on minimisation of control effort for class of underactuated system was proposed by (Farahani, Suratgar and Talebi, 2013), the technique performance was assessed using simulation based and a comparison study was conducted to the broadly utilized strategies for control of capsubot open-loop and close-loop control and the outcomes was promising , however this approach lacks the consideration of uncertainty of complex environment as well as experimental investigations ,as many cases the experimental results differs from simulation as it was observed in (Huda and Yu, 2015) the desired trajectory of experiment was not exactly as the simulation results, even though the method minimise energy consumption.

A study on modelling and dynamic analysis of capsule systems exhibiting the friction-induced hysteresis was introduced by (Liu et al. (2016)).

Moreover study on dynamic frictional of vibro-driven underactauted mechanical system with viscoelastic property was conducted in (Liu, Yu and Cang, 2019), it was discovered that the hysteric qualities affects the relative velocity basically during the pre-sliding and the effect of control parameters was likewise researched and it was discovered that a legitimate tuning of the parameters will bring about an improved system performance and avoidance of unwanted responses.

1.5.2 Frictions Models

1.5.2.1 The friction phenomena

The friction force is the reaction in the tangential direction between two contacting surfaces, in general friction can be described in two ways, static and dynamic friction and the difference between them is frictional memory (Wojewoda et al., 2007). Understanding the characteristics and features of friction is very important, in order to understand and analyse existing friction models, friction features varies and they are non-linear in nature and the performance of the friction is determined by its ability to replicate these observed phenomena in a better way and closely. Some of the friction characteristics are stick-slip motion, pre-sliding hysteresis, frictional lag, break-away and varying break-away forces and stribeck affect (Nnaji, 2017).

1.5.2.2 Classical friction models

The classical friction model is made up with various components that individually capture various aspects of the friction and the components of this models are coulomb, viscous, stribeck friction and static.

Coulomb friction

The coulomb's friction states that the friction is proportional to normal loading between the two surfaces and operates in the same way to oppose the bodies on motion. Mathematically the coulomb's friction can be described as following

$$F_f = \mu_C N sgn(\dot{\boldsymbol{x}}) \tag{2.1}$$

And in terms of coulombs friction $F_C = \mu_C N$

$$F_f = F_C sgn(\dot{\boldsymbol{x}}) \tag{2.2}$$

Where F_f friction force, N normal loading, μ_C kinetic friction coefficient, $\dot{x}$ relative velocity and F_C coulomb's friction force .However, the coulomb's only takes on two values of the same magnitude which depends on the direction of motion but it does not capture the friction phenomena dynamic in zero velocity.

Viscous friction

The viscous friction simply proportional to the velocity of motion and increase when the velocity increase and decrease when velocity decrease and the vicious friction coefficient is quite small due to viscosity and it can be very small in low velocities, therefor the viscous friction often appears to be modelled as linear function of velocity as it is shown in equation (2.3).Usually the viscous friction is incorporated with coulomb friction as it shown in equation (2.4) ,(Beauchamp, 1886).

$$F_f = f_v \dot{\boldsymbol{x}} \tag{2.3}$$

$$F_f = F_C sgn(\dot{\boldsymbol{x}}) + f_v v \tag{2.4}$$

Where f_v is the viscous friction coefficient and from equation 2.4 we observe that during sliding the friction force is the sum of both frictions.

Static friction

The static friction is the amount of friction required to start or initiate motion and its stiction values depend on the applied force and does not depend on the velocity and the main concept of this friction force is independent of the body in motion contact area and velocity and it increases with the force till the breakaway force is reached and mathematically is described by equation (2.5).

$$F_S = \mu_S N \tag{2.5}$$

Where F_S is the static friction and μ_S the static friction coefficient.

Stribeck friction model

The stribeck friction model or the stribeck curve represents the curve in which the transition friction from static to coulombs of kinetic friction and the stribeck is represented by exponential function as it is shown in (2.6)

$$F_f = F_C sgn(\dot{\boldsymbol{x}}) + (F_S - F_C)\boldsymbol{e}^{-\left(\frac{\dot{x}}{v_s}\right)^{\delta}} \tag{2.6}$$

Where v_S is the stribeck or transition velocity and δ curve shaping. Furthermore classical friction models are the karnop model, Lorinic model and neural network based model.

1.5.2.3 Dynamic friction models

In the previous section it was seen that the static friction models lack the detection of the friction dynamic in the presiding because they are static mapping of force as function of velocity and not displacement or position, for many systems has effects of non-linearity's mainly in pre-sliding and cause errors and due to these factors, it is highly needed an accurate friction models that describes some dynamism. Therefore, the friction models that reproduce the friction features in this regime are modelled as function of velocity and the internal state of surface in contact and these models are called dynamic friction models whose are more complex and some of these models are Dahl, Bristle, LuGree, GMS, Leuven and Xiong (Nnaji, 2017) however in this thesis the LuGree friction is under consideration for dynamic modelling of capsubot class of underactuated mechanical system.

LuGree model

The LuGree friction in an improvement of Dahl model with more features and it was proposed by(Olsson, Astrom, deWit and Liscinsky, 1995) and it was improved by (Lampaert, Swevers and Al-Bender, 2002) and improvement was made by the integrated friction Leuven, the improvement was in reformulating the non-linear state equation and was done for the purpose of always obtaining a continues friction and the improvement was to solve the stack overflow which occur in the hysteresis and the mathematical representation of the LuGree friction is shown below,

$$F_f = \sigma_0 Z + \sigma_1(v)\dot{Z} + \sigma_2(v) \tag{2.7}$$

$$\dot{Z} = \left(V - \left(\frac{|(v)|}{g(v)}\right) Z\right) \tag{2.8}$$

$$g(v) = \frac{1}{\sigma_0}\left(f_C + (f_S - f_C)e^{-\left(\frac{v}{v_S}\right)^2}\right) \tag{2.9}$$

Where F_f represents the LuGree friction, σ_0 the stiffness of the used material, Z the bristle deflection, v_S is the stribeck velocity, σ_1 the material damping coefficient, $g(v)$ the non-linear model of the stribeck at low velocity, v is the relative velocity, $\sigma_2$is viscous damping coefficient.

Bristle, Dahl, Leuven, MS and Xiong Model

This section briefly will review the bristle, Dahl, Leuven, GMS and Xiong friction models as they will not be used in modelling the capsubot system under consideration.

The Dahl model was proposed by (Dahl, 1968) and this friction model was mainly designed to capture the friction phenomena in the presiding region and is governed mathematically by equation (2.10).

$$\frac{dF_f}{dt} = \sigma\left(1 - \frac{F_f}{F_C}(\dot{Z})\right)^{\delta} \tag{2.10}$$

Where $\frac{dF_f}{dt} = \frac{dF_f}{dt}\frac{dZ}{dt}$ and $\dot{Z} = v - \sigma\left(\frac{|v|}{F_C}Z\right)$ then $F_f = \sigma Z$

The Bristle friction model is given by the mathematical equation () and it was proposed by (Haessig and Friedland 1991).

$$F_f = KZ \tag{2.11}$$

Where Z = (x-y) which is the bristle deflection and K as the bristle stiffness and it depends in the number of bristle element and the total friction force is given by.

$$F_f = \sum_{i=1}^{n} K_i Z_i \qquad \text{And} \quad i = 1\,,2\,,3\; n$$

For the Leuven, GMS and Xiong mathematical governing equations and proofs are provided in (AI-Bender and Swevers, 2000), (AI-Bender and Swevers, 2003) and (Xiong, Kikuuwe and Yamamoto, 2013) respectively.

Friction in Control system Application

It is very important in control engineering to understand the system we dealing with behaviour and in order to understand the system behaviour is to have it modelled with friction models and this can assist the design strategies of control that can help to evaluate the system performance due to friction, an example of system in interest such as simple devices in standard control loops with valves and more complex precision system such as radar, telescope and robots for accurate pointing (Olsson et al., 1998) .

1.6 Needs and Challenges of Medical Applications Robots

1.6.1 Needs of Medical robotics

Robotics are showing huge effect to medicine and nowadays medical robots are used in difference sectors of medicine such as performing surgery, delivering physical and occupational therapy and furthermore can be used to collect data in biological systems(Okamura et al. 2010). The needs of medical robots can be seen from various point of view such as patients, medicine professionals (doctors, nurses), hospitals, companies and researchers (Huda, 2019).

1.6.2 Challenges of medical robots

The challenges of medical robots can be seen from different point of view such cost, safety, energy consumption, speed, size and weight, stopping/anchoring capability. Some of the challenges with external large robots are, the weight and to make light and adding flexibility to the system (Marcus et al. 2013).Laparoscopic robots have seen a huge development in the past decade with overall good results, despite its expansion is not the chosen approach yet due to many factor such as the camera instability, its instruments and in the other hand the cost (Li and Chiu 2018). As it is shown in figure (2.1) and (2.2), the robots consist external parts which can be a risk to patient safety.

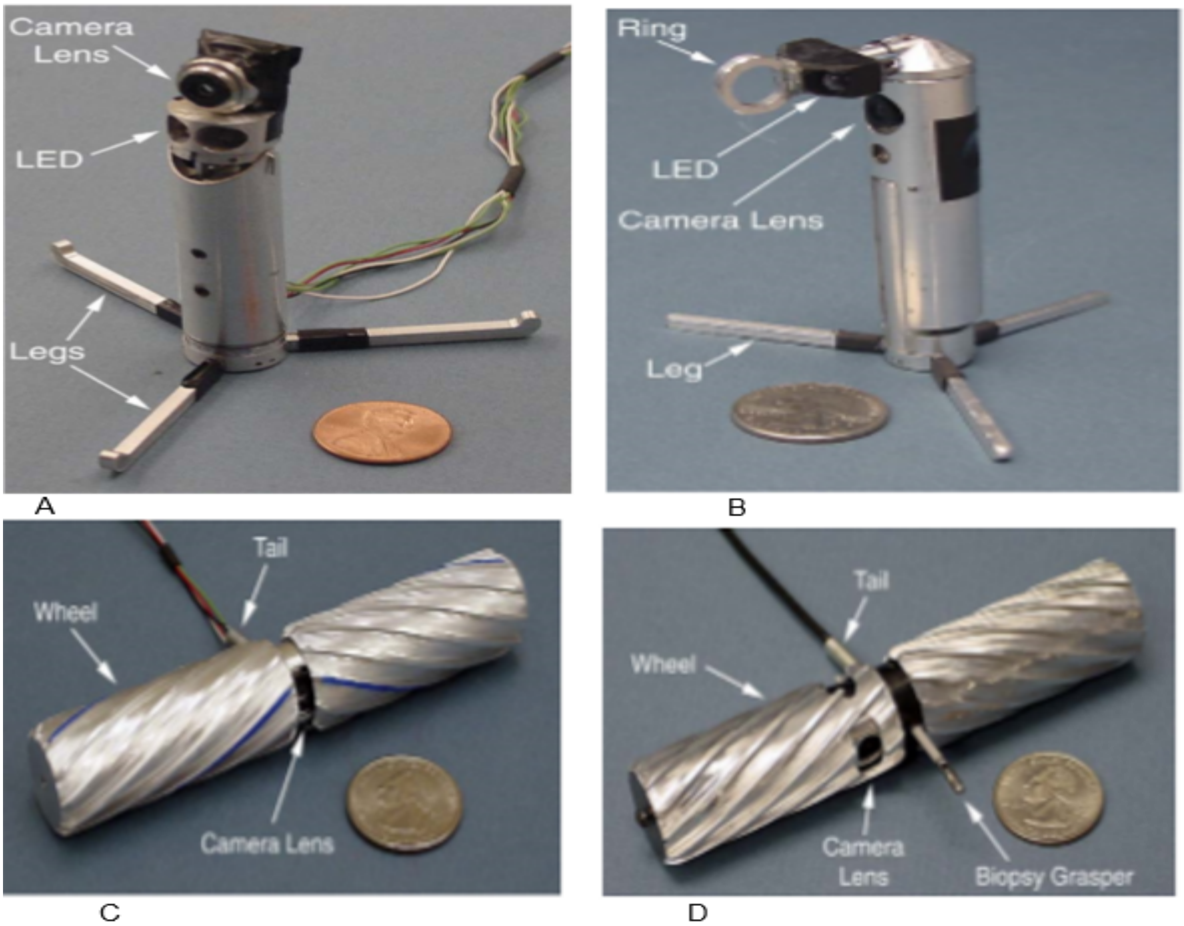

Figure 0.1 Examples of In vivo laparoscopic robots (Rentschler et al., 2006)

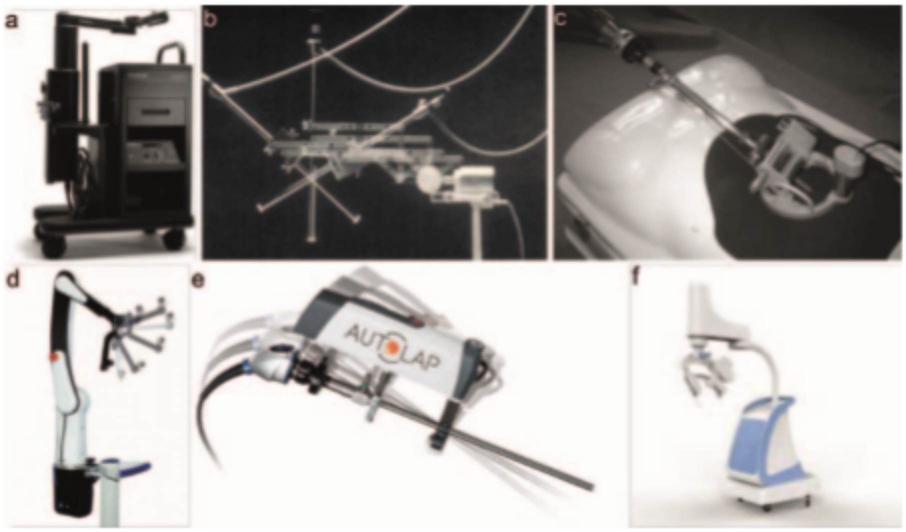

Figure 0.2 examples of robot-assisted endoscopy rigid **(Li and Chiu 2018)**

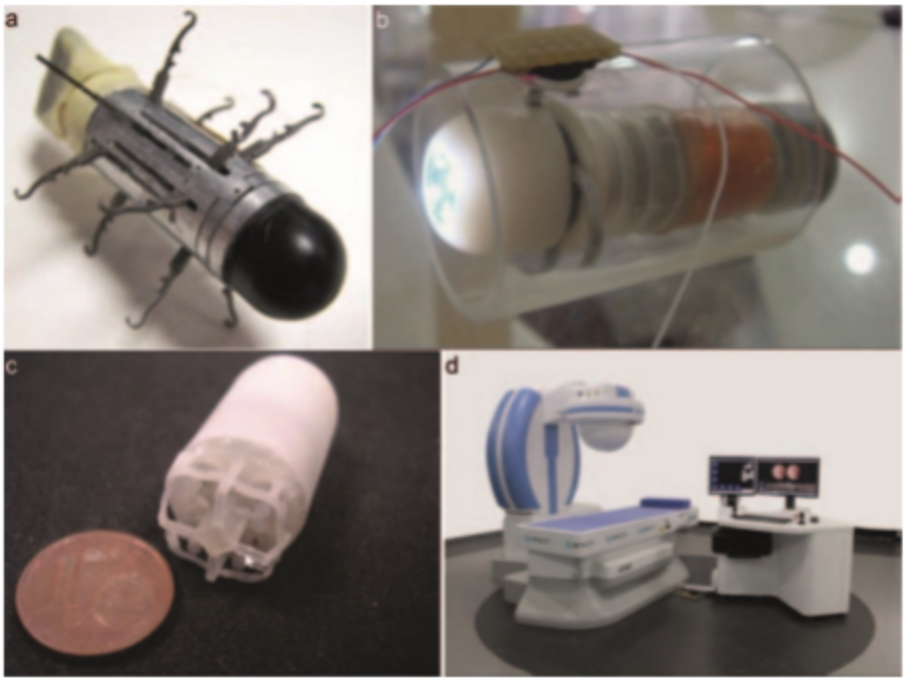

Figure 0.3 examples of active capsule and in vivo robots **(Li and Chiu 2018)**

As it is shown above in the figures above, samples of existing medical robots are presented , in figure (2.1) four examples of in vivo laparoscopic robots are presented which contains external parts and figure (2.2) a robot-assisted endoscopy rigid and in figure (2.3) and capsule and in vivo robots.

1.7 Dynamic Modelling of underactuated Mechanical system

Representing a system in mathematical form is very important and it is very important that the right mathematical way of representing a system to be chosen. The system under consideration in this thesis is 1D capsule robot (capsubot) and it is a class of underactuated mechanical system, therefore, in this section some of the methods that appeared in literature review for modelling underactuated mechanical system will be presented.

1.7.1 Newton Second law of motion in terms of differential equation

The classical and simplest way to model a mechanical system is in the form of differential equation using the newton second law, for simplicity let's consider the mechanical system of mass-spring-damper with single degree of freedom shown in figure (2.4). Using newton second law of motion the differential equation that represent the mass-spring-damper system is as following

$$F(t) = M\ddot{X}(t) + C\dot{X}(t) + KX(t) \tag{2.12}$$

Where X (t) is the position of the mass, M is the mass (Kg), K is the spring constant (N/m), C is the damping coefficient (N s/m) and F (t) is the input force (N)

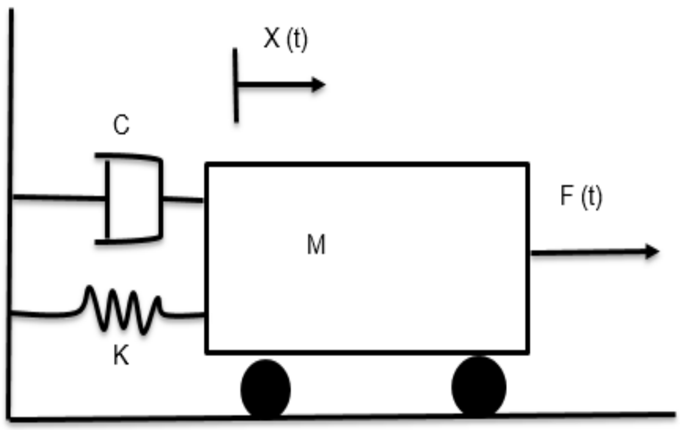

Figure 0.4 schematic diagram of mass-spring-damper systems

1.7.2 The Euler-Lagrange method

Based on (Olfati-Saber, 2001) an underactuated mechanical systems can be represented as following using the Euler-Lagrange equation of motion

$$\frac{d}{dt}\frac{\partial \mathcal{L}}{\partial \dot{q}} - \frac{\partial \mathcal{L}}{\partial q} = F(q)\tau \qquad (2.13)$$

Where $F(q) \in R_{n\times m}$, is the non-square matrix of the external forces with $m < n$ and $\tau \in R^{m}$ is the control, m represents the number of control inputs which less than n, which is configuration variable. For a simple lagrangian system, the underactuated mechanical system equation of motion can be expressed as such

$$M(q)\ddot{q} + C(q, \dot{q})\dot{q} + G(q) = F(q) \qquad (2.14)$$

And the configuration vector can be partitioned as following $q = (q_1, q_2) \in R^{(n-m)} \times R^{m}$ by assuming $F(q) = [0, I_m]^T$ and according to $F(q)$ q_1 and q_2 represents the configuration vectors actuated and unactuated respectively and after partitioning the inertia matrix M(q) the underactuated mechanical system dynamic can be represented as following

$$\begin{bmatrix} m_1(q) & m_3(q) \\ m_2(q) & m_4(q) \end{bmatrix} \begin{bmatrix} \ddot{q_1} \\ \ddot{q_2} \end{bmatrix} + \begin{bmatrix} h_1(q, \dot{q}) \\ h_2(q, \dot{q}) \end{bmatrix} = \begin{bmatrix} 0 \\ \tau \end{bmatrix} \qquad (2.15)$$

Due to the lack of control input in the first equation of (2.14), the chances of fully linearizing it, is not possible , however it is still possible to partially linearize it , the dynamic of q_2 transforms to double integral.

1.7.3 The state-space representation

The sate-space representation can be deriven either from the system model given by continues-time differential equation or from its transfer function, for example let's consider the mass-spring-damper described by equation (2.12).

The state variables of the system are X (t) which is the displacement and its first and second derivative $\dot{X}(t)$ which is the velocity and $\ddot{X}(t)$ which is the acceleration.

Let's rename our state-space variables

$$x_1(t) = \mathrm{X}\,(\mathrm{t}) \ , x_2(t) = \dot{X}(t) = \dot{x}_1(t)$$

From the above configuration we observe that $x_1(t)$ is the displacement of the mass and $x_2(t)$ is the velocity, therefore

$$\dot{x}_2(t) = \ddot{X}(t)$$

And from the change of variable we obtain our first order differential equation as following

$$\dot{x}_1(t) = x_2(t) \tag{2.16}$$

And making a substitution we get that

$$\mathrm{F}\ (\mathrm{t}) = \mathrm{M}\dot{x}_2 + \mathrm{C}x_2 + \mathrm{K}x_1 \tag{2.17}$$

Rearranging (2.17) leads to the first order differential equation

$$\dot{x}_2 = \frac{F}{M} - \frac{C}{M}x_2 - \frac{K}{M}x_1 \tag{2.18}$$

And now from equation (2.16) and (2.18) we can derive the state-space matrix representation as such

$$\begin{bmatrix} \dot{x}_1 \\ \dot{x}_2 \end{bmatrix} = \begin{bmatrix} 0 & 1 \\ -\frac{K}{M} & -\frac{C}{M} \end{bmatrix} \begin{bmatrix} x_1 \\ x_2 \end{bmatrix} + \begin{bmatrix} 0 \\ \frac{1}{M} \end{bmatrix} F \tag{2.19}$$

$$y = \begin{bmatrix} 1 & 0 \end{bmatrix} \begin{bmatrix} x_1 \\ x_2 \end{bmatrix} \tag{2.20}$$

Where (2.19) is the state equation and (2.20) is the output equation.

$$\dot{x}_1 = Ax + Bu$$

$$y = Cx + Du$$

Where A, B, C, D are the matrixes and D is zero for most cases and F is the control input.

1.8 Chapter Summary

The literature review has presented different perspective of medical robots, such as needs and challenges of medical robots, as the art of literature review stated, the demand on medical robots is very high, despite the cost, complexity and performance, the robot under consideration on this research is a 1D capsule robot, which is underactuated mechanical, (the capsubot) has no external parts, whereas most of the other medical robots consist of external parts , however , the main challenge with the robot under consideration is controlling , the trajectory tracking due to its mechanical system , different approaches was developed for control of class of underactuated mechanical system but a novel approach was proposed by (Huda and Yu, 2015), which is two stage control and both simulation and experimentation investigation was conducted based in open loop control system approach.

Also in this chapter a different friction models was reviewed and stated in terms features, the friction models that has been reviewed are static model and dynamic models .As the art of literature review stated, choosing the most appropriate friction model for the purpose of modelling system is very important, therefore, a different friction models will be used to model a class of underactuated mechanical system and investigated.

1.9 Scope of contribution

The capsubot have potential to make engineering and medical diagnosis process, however as the art of literature review suggest more researches are required to release a capsubot with high accuracy and good performance.

The limitation of controlling the trajectory tracking of a capsubot in the literature justify the needs of designing and developing a control strategy for highly accurate medical capsubot. Therefore, this research will investigate a close-loop control for class of underactuated mechanical system. The method under consideration is, the method proposed by (Huda and Yu, 2015), The feedback linearization was successfully in many cases of underactuated mechanical system and it will be used within the inner mass control .This research also will propose different approach of describing the friction phenomena by modelling the system with an advanced friction model

The capsubot is also a non-linear system and this thesis will also propose a way of linearizing the capsubot model. The proposed linearization method will be based on replacing the scaler sign function by approximated function and then conducting the linearization.

Chapter Three

1.10 Dynamic modelling

The schematic diagram shown in figure (3.1), is the dynamic modelling of 1D capsule robot (capsubot). The inner mass can move from one end to another end, and by controlling the inner mass, the capsubot movement can be achieved to the desired direction, in the schematic below the source of the propulsion force is not presented.

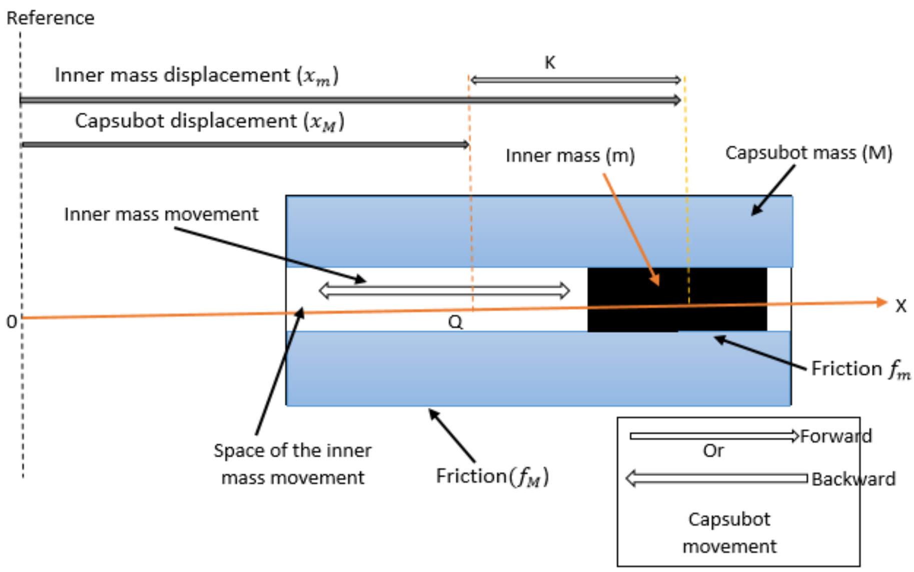

Figure 0.1:Schematic diagram of 1D capsubot

The movement of the capsubot depends on the applied force to the inner mass which is F_{IM} and the dynamical representation of the capsubot mathematically is. (Huda and Yu, 2015).

$$F_{IM} = \mathrm{m}\ddot{x}_m + f_m \tag{3.1}$$

$$F_{cap} = -\mathrm{m}\ddot{x}_m + f_m = \mathrm{M}\ddot{x}_M + f_M \tag{3.2}$$

Where

- F_{IM} and F_{cap} are the force applied to the inner mass and force received by capsubot.
- M and m are the masses of the capsubot and IM respectively.
- $\ddot{x}_M$ and $\ddot{x}_m$ the displacements of the capsubot and IM respectively. By

1.10.1 Capsubot dynamic modelling with Coulomb Friction Model

By using the coulomb's friction principles (Olsson et al., 1998), the friction can be defined as $F_{friction}$ =$\beta(\dot{x})\mu mg$ and $\beta(\dot{x})$ can be adopted as such $\beta(\dot{x})$ = sgn($\dot{x}$) and equations (3.1) and (3.2) can be rewritten as following

$$F_{IM} = \mathrm{m}\ddot{x}_m + sgn(\dot{x}_{IM} - \dot{x}_{cap})\mu_{IM}mg \tag{3.3}$$

$$F_{cap} = \mathrm{M}\ddot{x}_M + sgn(\dot{x}_{cap})\mu_{cap}Mg \tag{3.4}$$

- $\dot{x}_{IM}$ and $\dot{x}_{cap}$ are the IM and capsubot velocities respectively;
- μ_{IM} and μ_{cap} are the coulomb's coefficients which corresponds to f_m and f_M respectively.

1.10.1.1 State-space representation with coulomb friction model

The state-space representation for (3.3) and (3.4) can be obtained using the same method used in section (2.3.3) and therefore the stat-space representation for the capsubot with coulomb friction model friction model is as following

Capsubot State-space representation

From (3.4) the state variables of the system are $\mathrm{x_{cap}}$ which is the displacement of the capsubot, $\mathrm{\dot{x}_{cap}}$ is the velocity of the capsubot and $\mathrm{\ddot{x}_{cap}}$ is the acceleration of the capsubot and renaming the state variables we obtain the following

$$\mathrm{x_{cap}} = \mathrm{x_1}\,,\ \mathrm{\dot{x}_{cap}} = \mathrm{x_2} \text{ and } \mathrm{\dot{x}_2} = \mathrm{\ddot{x}_{cap}}$$

And from the above change of variables we obtain a first ODE as following

$$\mathrm{\dot{x}_1} = \mathrm{x_2} \tag{3.5}$$

Making substitution to (3.4) we obtain

$$F_M = -m\dot{x}_4 = -m[-sgn(x_4 - x_2)\mu_m mg + (1/m)u] \tag{3.6}$$

Rearranging (3.6) making the acceleration the subject we obtain our second, first ODE for the capsubot acceleration as following

$$\dot{x}_2 = \frac{1}{M}((-m[-sgn(x_4 - x_2)\mu_m mg + (1/m)u]) - sgn(x_2)\mu_M Mg) \tag{3.7}$$

Inner Mass State-space representation

These from (3.3) the state variables for the inner mass arex_{IM} , $\dot{x}_m$ and $\ddot{x}_m$ describing the displacement, velocity and acceleration of the inner mass, and renaming the state variables we get

$$x_m = x_3 , \dot{x}_m = x_4 , \dot{x}_4 = \ddot{x}_m$$

Therefore, from the above renaming our first equation in terms of first order differential equation is as following

$$\dot{x}_3 = x_4 \tag{3.8}$$

And making substitution into (3.4) we obtain the second equation as such

$$F_{IM} = m\dot{x}_4 + sgn(x_4 - x_2)\mu_m mg$$

Rearranging the above equation making the acceleration subject

$$\dot{x}_4 = \frac{1}{m}(F_m - sgn(x_4 - x_2)\mu_m mg) \tag{3.9}$$

Using the state-space representation, the two second order differential equations that describes the capsubot and inner mass (3.3) and (3.4) has been reduced to first order differential equations represented by (3.7) and (3.9) respectively.

1.10.2 Capsubot and Inner Mass dynamic modelling with LuGree Friction Model

As is shown in section (3.1.1) the capsubot and Inner mass dynamic with coulombs friction, in this section a dynamic of the capsubot and inner mass with LuGree friction is presented.

1.10.2.1 Capsubot Dynamic modelling with LuGree friction

The capsubot system represented by (3.2) can modelled as following using the LuGree friction model described by (2.7), (2.8) and (2.9) as following,
Recalling (3.2)

$$F_{cap} = \text{-m}\ddot{x}_m + f_m = \text{M}\ddot{x}_M + f_M$$

Where F_{cap} is the force received by the capsubot, M capsubot mass, $\ddot{x}_M$ capsubot acceleration and f_M the friction phenomena between the capsubot shell and the surface of motion. Replacing f_M by (2.7) we obtain the capsubot model describing its friction with the LuGree friction model as following

$$F_{cap} = -m\dot{x}_4 = M\ddot{x}_{cap} + \sigma_{0\_cap}Z_{cap} + \sigma_{1\_cap}\dot{Z}_{cap} + \sigma_{2\_cap}(\dot{x}_{cap}) \tag{3.10}$$

Where

$$\dot{Z}_{cap} = \left((\dot{x}_{cap}) - \left(\frac{|(\dot{x}_{cap})|}{g(\dot{x}_{cap})} \right) Z_{cap} \right) \tag{3.11}$$

And

$$g(\dot{x}_{cap}) = \frac{1}{\sigma_{0\_cap}} \left(f_{c\_cap} + (f_{s\_cap} - f_{c\_cap}) e^{-\left(\frac{\dot{x}_{cap}}{v_{sc}}\right)^2} \right) \tag{3.12}$$

$$f_{c\_cap} = sgn(\dot{x}_{cap})\mu_{cap}Mg \tag{3.13}$$

Where $\dot{\boldsymbol{x}}_{\boldsymbol{cap}}$ denotes the capsubot velocity, $\ddot{x}_{cap}$ denotes the capsubot acceleration, $f_{s_cap}$the static friction , f_{c_cap} coulomb friction ,σ_{0_cap} the stiffness of the used material, $\boldsymbol{Z_{cap}}$ the bristle deflection, v_{SC} is the stribeck velocity, σ_{1_cap} the material damping coefficient $\boldsymbol{g}(\dot{\boldsymbol{x}}_{\boldsymbol{cap}})$ **is** the non-linear model of the stribeck at low velocity, $\sigma_{2_cap}$is viscous damping coefficient, μ_{cap} is the coulombs friction coefficient for capsubot.

1.10.2.2 Inner Mass Dynamic modelling with LuGree friction

In section (3.1.1) the inner mass was modelled with coulomb friction, therefore in this section the inner mass is modelled with the LuGree friction as such, replacing the f_m in (3.1) by the LuGree friction model given in (2.7) we obtain

$$F_{IM} = m\ddot{x}_{IM} + \sigma_{0IM}Z_{IM} + \sigma_{1IM}\dot{Z}_{IM} + \sigma_{2IM}(\dot{x}_{IM} - \dot{x}_{cap}) \tag{3.14}$$

Where
$$\dot{Z}_{IM} = (\dot{x}_{IM} - \dot{x}_{cap}) - \frac{|\dot{x}_{IM} - \dot{x}_{cap}|}{g(\dot{x}_{IM} - \dot{x}_{cap})} Z_{IM} \tag{3.15}$$

And

$$g(\dot{x}_{IM} - \dot{x}_{cap}) = \frac{1}{\sigma_{0\_IM}} \left(f_{c\_IM} + (f_{s\_IM} - f_{c\_IM}) e^{-\left(\frac{\dot{x}_{IM} - \dot{x}_{cap}}{v_{sm}}\right)^2} \right) \tag{3.16}$$

$f_{c\_IM} = sgn(\dot{x}_{IM} - \dot{x}_{cap})\mu_{IM}mg$ Coulombs friction corresponding to IM

IM denotes inner mass, therefore σ_{0_IM} denotes the stiffness of the material, f_{s_IM} static friction, f_{c_IM} is the coulombs friction, Z_{IM} is the bristle deflection, v_{Sm} is the stribeck velocity, σ_{2IM} is viscous coefficient, $g(\dot{x}_{IM} - \dot{x}_{cap})$ is the non-linear model at low velocity all corresponding to inner mass respectively.

1.10.3 State-space representation with LuGree friction model

1.10.3.1 State-space representation for capsubot with LuGree friction model

The state-space representation for the capsubot with LuGree friction is the same procedure except in this section the friction phenomena will be described by the LuGree friction model for accuracy purposes and capturing more friction phenomena at low velocity and the LuGree friction has these features, in order to do the state-space representation for the model described by (3.10), first we need to state the state variables of the system , therefore , the state variables of the system of (3.10) are x_{cap} which is the capsubot displacement and its first and second derivative $\dot{x}_{cap}$ and $\ddot{x}_{cap}$ which correspond to the capsubot velocity and acceleration respectively, another states are Z_M and $\dot{Z}_M$.

Renaming the state variables to reduce order of derivative we obtain the following

$$x_{cap} = x_1 , \dot{x}_{cap} = x_2 , \dot{x}_2 = \ddot{x}_{cap} , x_3 = Z_{cap} , \dot{x}_3 = \dot{Z}_{cap}$$

Therefore, the first derivative of x_1 equals to x_2 from that our first ODE which is first order as such

$$\dot{x}_1 = x_2 \tag{3.17}$$

And making substitution into (3.10) replacing the state variables, using renamed equivalent variables we obtain

$$F_{cap} = -m\dot{x}_4 = M\dot{x}_2 + \sigma_{0\_cap}x_3 + \sigma_{1\_cap}\dot{x}_3 + \sigma_{2\_cap}x_2 \tag{3.18}$$

Where $$\dot{x}_3 = x_2 - \frac{|x_2|}{g(x_2)}x_3 \tag{3.19}$$

Then $$g(x_2) = \frac{1}{\sigma_{0\_cap}}\left(f_{c\_cap} + (f_{s\_cap} - f_{c\_cap})e^{-\left(\frac{x_2}{v_{sc}}\right)^2}\right) \tag{3.20}$$

And coulombs friction

$$f_{c\_cap} = sgn(x_2)\mu_M Mg \tag{3.21}$$

Rearranging (3.18) making the acceleration the output we obtain our second ODE as following

$$\dot{x}_2 = \frac{1}{M}\left(-m\dot{x}_4 - \sigma_{0\_cap}x_3 - \sigma_{1\_cap}\left(\sigma_{1\_cap}(x_2 - \frac{|x_2|}{g(x_2)}x_3\right) - \sigma_{2\_cap}x_2\right) \tag{3.22}$$

Where $\dot{x}_5$ can be determined by (3.27)

1.10.3.2 State-space representation for inner mass with LuGree friction model

In order to obtain the state-space representation for the inner mass model, let's start by stating our state variables from (3.14) and by doing so we get our state variables as such x_{IM} denotes the inner mass displacement and its first and second derivative $\dot{x}_{IM}$ *and* $\ddot{x}_{IM}$ which describes the inner mass velocity and acceleration respectively , the other state variables are Z_{IM} and $\dot{Z}_{IM}$.
Renaming the state variables, we get

$$x_{IM} = x_4 , \dot{x}_{IM} = x_5 , \dot{x}_{IM} = \ddot{x}_{IM} , x_6 = Z_{IM} , \dot{x}_6 = \dot{Z}_{IM}$$

And from the above renaming process we observe that $\dot{x}_4$ equalsx_5 , therefore we obtain our first ODE as such

$$\dot{x}_4 = x_5 \tag{3.23}$$

And making substitution into (3.14) we obtain

$$F_m = m\dot{x}_5 + \sigma_{0\_IM}x_3 + \sigma_{1\_IM}(x_5 - x_2) - \frac{|(x_5-x_2)|}{g(x_5-x_2)}x_6 + \sigma_{2_{IM}}(x_5 - x_2) \tag{3.24}$$

Where $$g(x_5 - x_2) = \frac{1}{\sigma_{0\_IM}}\left(f_{c\_IM} + (f_{s\_IM} - f_{c\_IM})e^{-\left(\frac{(x_5-x_2)}{v_{sm}}\right)^2}\right) \tag{3.25}$$

And $$f_{c\_IM} = sgn(x_5 - x_2)\mu_m mg \tag{3.26}$$

And rearranging (3.24) making the inner mass acceleration the subject we obtain

$$\dot{x}_5 = \frac{1}{m}\left(F_{IM} - \sigma_{0\_IM}x_6 - \sigma_{1\_IM}\left(\sigma_{1\_IM}((x_5 - x_2) - \frac{|(x_5-x_2)|}{g((x_5-x_2))}x_6\right) - \sigma_{2\_IM}(x_5 - x_2)\right) \tag{3.27}$$

1.10.4 Capsubot and Inner Mass dynamic modelling with Stribeck Friction Model

Replacing the f_M and f_m in (3.2) and (3.1) with the stribeck friction model represented by (2.6), (3.2) and (3.1) can be rewritten as following

$$F_{cap} = \mathrm{M}\ddot{x}_{cap} + sgn(\dot{x}_{cap})\mu_M Mg + (F_{S\_cap} - F_{C\_cap})\boldsymbol{e}^{-\left(\frac{\dot{x}_{cap}}{v_{sc}}\right)^{\delta}} \tag{3.28}$$

$$F_{IM} = \mathrm{m}\ddot{x}_{IM} + sgn(\dot{x}_{IM-}\,\dot{x}_{cap})\mu_M mg + (F_{S\_cap} - F_{C\_cap})\boldsymbol{e}^{-\left(\frac{\dot{x}_{IM}-\dot{x}_{cap}}{v_{sm}}\right)^{\delta}} \quad (3.29)$$

1.10.5 State-space representation with stribeck friction model

Using the same procedure the sate-space representation for this model (3.28) and (3.29) can be rewritten as following

State variables for (3.28) $x_{cap} = x_1$, $\dot{x}_{cap} = x_2$, $\dot{x}_2 = \ddot{x}_{cap}$

State variables for (3.29) $x_{IM} = x_3$, $\dot{x}_{IM} = x_4$, $\dot{x}_4 = \ddot{x}_{IM}$

State equations for capsubot are

$$\dot{x}_1 = x_2 \quad (3.30)$$

$$F_{cap} = \mathrm{M}\dot{x}_2 + sgn(x_2)\mu_M Mg + (F_{S\_cap} - F_{C\_cap})\boldsymbol{e}^{-\left(\frac{x_2}{v_{sc}}\right)^{\delta}}$$

Rearranging the above equation making $\dot{x}_2$ we obtain

$$\dot{x}_2 = \frac{1}{M}(F_{cap} - sgn(x_2)\mu_M Mg - (F_{S\_cap} - F_{C\_cap})\boldsymbol{e}^{-\left(\frac{x_2}{v_{sc}}\right)^{\delta}} \quad (3.31)$$

State equations for inner mass are

$$\dot{x}_3 = x_4 \quad (3.32)$$

$$\dot{x}_4 = \frac{1}{m}(F_{IM} - sgn(x_4 - x_2)\mu_m mg - (F_{IM} - F_{IM})\boldsymbol{e}^{-\left(\frac{x_4}{v_{sc}}\right)^{\delta}} \quad (3.33)$$

1.11 Proposed linearization

In systems dynamic modelling , we see that most systems are non-linear , which means the differential equation governing the system's evolution is non-linear , an example of such systems is the capsubot the system under consideration on this thesis .However ,most theories that have been developed are based on linear systems. In order to view the non-linear model of the capsubot as a linear model we need develop what's called the Jacobean linearization around equilibrium point.

Equilibrium point

Let's consider the non-linear differential equation below

$$\dot{x}(t) = f(x(t), u(t)) \quad (3.34)$$

Where f is the function that maps $R^n \times R^m \to R^n$. The point $\bar{x} \in R^n$ is the equilibrium point and $\bar{u} \in R^m$ is the equilibrium input.

The system we are dealing with on this thesis consist of sign function and absolute which cannot be differentiated straight away as the Jacobean linearization is based on partial derivative evaluation around equilibrium point. An approximated scaler function was introduced by (Zhang et al. 2011) , which is shown below

$$sgn(x) = \frac{(1+x)^k-(1-x)^k}{(1+x)^k+(1-x)^k} \tag{3.35}$$

$$|x| = x\, sgn(x) \approx x\, sgn_K(x) \tag{3.36}$$

$$\frac{d(sgn)}{dx} = \frac{4k(1-x^2)^{k-1}}{\left[(1+x)^k+(1-x)^k\right]^2} \tag{3.37}$$

1.11.1 Linearizing system with coulombs friction model

Replacing the sgn function with (3.35) and rewriting (3.7) to linearize the system with coulombs friction model we get

$$\dot{x}_2 = \frac{1}{M}((-m[-\left(\frac{4k(1-x_4{}^2)^{k-1}}{\left[(1+x_4)^k+(1-x_4)^k\right]^2} - \frac{4k(1-x_2{}^2)^{k-1}}{\left[(1+x_2)^k+(1-x_2)^k\right]^2}\right)\mu_m mg + (1/m)u]) - \frac{4k(1-x_2{}^2)^{k-1}}{\left[(1+x_2)^k+(1-x_2)^k\right]^2}\mu_M Mg) \tag{3.38}$$

$$\dot{x}_1 = x_2 = f_1(x_2)$$

$$\dot{x}_3 = x_4 = f_3(x_4)$$

$$\dot{x}_4 = \frac{1}{m}\left(F_m - \left(\frac{4k(1-x_4{}^2)^{k-1}}{\left[(1+x_4)^k+(1-x_4)^k\right]^2} - \frac{4k(1-x_2{}^2)^{k-1}}{\left[(1+x_2)^k+(1-x_2)^k\right]^2}\right)\mu_m mg\right) = f_4(x_2, x_4, u)$$

Therefore, using the Jacobean linearization methods

$$\dot{x}_1 = f_1(x_1,u) + \frac{\partial f_1}{\partial x_1}\bigg|\frac{\delta x_1}{\overline{x_1}, \overline{u}} + \frac{\partial f_1}{\partial u}\bigg|\frac{\delta u}{\overline{x_1}, \overline{u}}$$

$$\dot{x}_2 = f_2(x_2,u) + \frac{\partial f_2}{\partial x_2}\bigg|\frac{\delta x_2}{\overline{x_2}, \overline{u}} + \frac{\partial f_2}{\partial u}\bigg|\frac{\delta u}{\overline{x_2}, \overline{u}}$$

$$\dot{x}_3 = f_3(x_3,u) + \frac{\partial f_3}{\partial x_3}\bigg|\frac{\delta x_3}{\overline{x_3}, \overline{u}} + \frac{\partial f_3}{\partial u}\bigg|\frac{\delta u}{\overline{x_3}, \overline{u}}$$

$$\dot{x}_4 = f_4(x_4, u) + \frac{\partial f_4}{\partial x_4}\bigg|\frac{\delta x_4}{\overline{x_4}, \bar{u}} + \frac{\partial f_4}{\partial u}\bigg|\frac{\delta u}{\overline{x_4}, \bar{u}}$$

And therefore, the Jacobean matrix for the coupled system will be in the form shown below

$$\dot{x} = \begin{bmatrix} \frac{\partial f_1}{\partial x_2} & \frac{\partial f_1}{\partial x_2} & \frac{\partial f_1}{\partial x_3} & \frac{\partial f_1}{\partial x_4} \\ \frac{\partial f_2}{\partial x_1} & \frac{\partial f_2}{\partial x_2} & \frac{\partial f_2}{\partial x_3} & \frac{\partial f_2}{\partial x_4} \\ \frac{\partial f_3}{\partial x_1} & \frac{\partial f_3}{\partial x_2} & \frac{\partial f_3}{\partial x_3} & \frac{\partial f_3}{\partial x_3} \\ \frac{\partial f_4}{\partial x_1} & \frac{\partial f_4}{\partial x_2} & \frac{\partial f_4}{\partial x_3} & \frac{\partial f_4}{\partial x_4} \end{bmatrix} \delta_x + \begin{bmatrix} \frac{\partial f_1}{\partial u} \\ \frac{\partial f_2}{\partial u} \\ \frac{\partial f_3}{\partial u} \\ \frac{\partial f_4}{\partial u} \end{bmatrix} \delta_u \qquad (3.39)$$

Assuming k=30 and taking the partial derivative and evaluating at equilibrium point we get the linear model for the capsubot coupled system with coulombs friction model

$$\dot{x} = \begin{bmatrix} 0 & 1 & 0 & 0 \\ 0 & -30\mu_M g & 0 & \frac{30\mu_m g m^2}{M} \\ 0 & 0 & 0 & 1 \\ 0 & 0 & -30\mu_m g & 30\mu_m g \end{bmatrix} \delta_x + \begin{bmatrix} 0 \\ \frac{1}{m} \\ 0 \\ \frac{1}{m} \end{bmatrix} \delta_u \qquad (3.40)$$

1.11.2 Linearizing system with LuGree friction model

$\dot{x}_1 = x_2 = f_1(x_2)$

Substituting (3.27) into (3.22) for $\dot{x}_5$ we get

$$\dot{x}_2 = \frac{1}{M}\left(-m(\frac{1}{m}\left(F_{IM} - \sigma_{0\_IM}x_6 - \sigma_{1\_IM}\left(\sigma_{1\_IM}((x_5 - x_2) - \frac{|(x_5-x_2)|}{g((x_5-x_2))}x_6\right) - \sigma_{2\_IM}(x_5 - x_2)\right)\right) - \sigma_{0\_cap}x_3 - \sigma_{1\_cap}\left(\sigma_{1\_cap}(x_2 - \frac{|x_2|}{g(x_2)}x_3\right) - \sigma_{2\_cap}x_2\right)$$

(3.41)

Replacing the absolute value by (3.36) and the sgn function by (3.35) thus (3.41) becomes

$$\dot{x}_2 = \frac{1}{M}\left(-m\left[\frac{1}{m}\left(F_{IM} - \sigma_{0_{IM}}x_6 - \sigma_{1_{IM}}\left(\sigma_{1_{IM}}((x_5 - x_2) - \frac{x_5\left(\frac{(1+x_5)^k-(1-x_5)^k}{(1+x_5)^k+(1-x_5)^k}\right)-x_2\left(\frac{(1+x_2)^k-(1-x_2)^k}{(1+x_2)^k+(1-x_2)^k}\right)}{g((x_5-x_2))}x_6\right) - \sigma_{2_{IM}}(x_5 - x_2)\right)\right] - \sigma_{0\_cap}x_3 - \sigma_{1\_cap}\left(\sigma_{1\_cap}(x_2 - \frac{|x_2|}{g(x_2)}x_3\right) - \sigma_{2\_cap}x_2\right) \quad (3.42)$$

For simplicity let's make 3.42 = $f_2(x_2, x_5, u)$ and when we are differentiating, we must take into account (3.20) and (3.21).

$$\dot{x}_3 = x_2 - \frac{|x_2|}{g(x_2)}x_3 \quad = \dot{x}_3 = x_2 - \frac{x_2\left(\frac{(1+x_2)^k-(1-x_2)^k}{(1+x_2)^k+(1-x_2)^k}\right)}{g(x_2)}x_3 \quad (3.42)$$

Where $g(x_2)$ is given by (3.20) and for simplicity let's make $\dot{x}_3 = f_3(x_2, x_3)$

$$\dot{x}_4 = x_5 = f_5(x_5) \quad (3.43)$$

$$\dot{x}_5 = \frac{1}{m}\left(F_{IM} - \sigma_{0\_IM}x_6 - \sigma_{1\_IM}\left(\sigma_{1\_IM}((x_5 - x_2) - \frac{x_5\left(\frac{(1+x_5)^k-(1-x_5)^k}{(1+x_5)^k+(1-x_5)^k}\right)-x_2\left(\frac{(1+x_2)^k-(1-x_2)^k}{(1+x_2)^k+(1-x_2)^k}\right)}{g((x_5-x_2))}x_6\right) - \sigma_{2\_IM}(x_5 - x_2)\right) = f_5(x_2, x_5, x_6, u) \quad (3.44)$$

$$\dot{x}_6 = (x_5 - x_2) - \frac{x_5\left(\frac{(1+x_5)^k-(1-x_5)^k}{(1+x_5)^k+(1-x_5)^k}\right)-x_2\left(\frac{(1+x_2)^k-(1-x_2)^k}{(1+x_2)^k+(1-x_2)^k}\right)}{g((x_5-x_2))}x_6 \quad (3.45)$$

$g((x_5 - x_2))$ is given by (3.25) and for simplicity lets make $\dot{x}_6 = f_6(x_2, x_5, x_6)$ and the linearized coupled system will be in the form of (3.46).

$$\dot{x} = \begin{bmatrix} \frac{\partial f_1}{\partial x_1} & \frac{\partial f_1}{\partial x_2} & \frac{\partial f_1}{\partial x_3} & \frac{\partial f_1}{\partial x_4} & \frac{\partial f_1}{\partial x_5} & \frac{\partial f_1}{\partial x_6} \\ \frac{\partial f_2}{\partial x_1} & \frac{\partial f_2}{\partial x_2} & \frac{\partial f_2}{\partial x_3} & \frac{\partial f_2}{\partial x_4} & \frac{\partial f_2}{\partial x_5} & \frac{\partial f_2}{\partial x_6} \\ \frac{\partial f_3}{\partial x_1} & \frac{\partial f_3}{\partial x_2} & \frac{\partial f_3}{\partial x_3} & \frac{\partial f_3}{\partial x_4} & \frac{\partial f_3}{\partial x_5} & \frac{\partial f_3}{\partial x_6} \\ \frac{\partial f_4}{\partial x_1} & \frac{\partial f_4}{\partial x_2} & \frac{\partial f_4}{\partial x_3} & \frac{\partial f_4}{\partial x_4} & \frac{\partial f_4}{\partial x_5} & \frac{\partial f_4}{\partial x_6} \\ \frac{\partial f_5}{\partial x_1} & \frac{\partial f_5}{\partial x_2} & \frac{\partial f_5}{\partial x_3} & \frac{\partial f_5}{\partial x_4} & \frac{\partial f_5}{\partial x_5} & \frac{\partial f_5}{\partial x_6} \\ \frac{\partial f_6}{\partial x_1} & \frac{\partial f_6}{\partial x_2} & \frac{\partial f_6}{\partial x_3} & \frac{\partial f_6}{\partial x_4} & \frac{\partial f_6}{\partial x_5} & \frac{\partial f_6}{\partial x_6} \end{bmatrix} \delta_x + \begin{bmatrix} \frac{\partial f_1}{\partial u} \\ \frac{\partial f_2}{\partial u} \\ \frac{\partial f_3}{\partial u} \\ \frac{\partial f_4}{\partial u} \\ \frac{\partial f_5}{\partial u} \\ \frac{\partial f_6}{\partial u} \end{bmatrix} \delta_u \qquad (3.46)$$

And assuming k =30 and taking the partial derivative of each function and evaluating at equilibrium point, we get

$$\dot{x} = \begin{bmatrix} 0 & 1 & 0 & 0 & 0 & 0 \\ 0 & \frac{1}{M}\left(-\sigma_{1_{IM}} - \sigma_{2\_cap}\right) & \frac{\sigma_{0\_cap}}{M} & 0 & \frac{1}{M}\left(-{\sigma_{1_{IM}}}^2 - \sigma_{2\_IM}\right) & \frac{\sigma_{0\_IM}}{mM} \\ 0 & 0 & 0 & 0 & 0 & 0 \\ 0 & 0 & 0 & 0 & 1 & 0 \\ 0 & \frac{1}{m}\left({\sigma_{1_{IM}}}^2 + \sigma_{2\_IM}\right) & 0 & 0 & \frac{1}{m}\left(-{\sigma_{1_{IM}}}^2 - \sigma_{2\_IM}\right) & \frac{-\sigma_{0\_IM}}{m} \\ 0 & 0 & 0 & 0 & 0 & 0 \end{bmatrix} \delta_x +$$

$$\begin{bmatrix} 0 \\ \frac{-1}{M} \\ 0 \\ 0 \\ \frac{1}{m} \\ 0 \end{bmatrix} \delta_u \qquad (3.47)$$

1.12 Acceleration profiles and Motion generation

1.12.1 Acceleration profiles

In order the capsubot to follow the desired trajectory, a trajectory tracking needs to be preformed and to do so , the four step acceleration profiles proposed in (Huda and Yu, 2015) .The acceleration profiles are the utorque and contrarium .The Utorque profile is a four-step acceleration and the contrarium is a two-step acceleration profile.

The Utorque acceleration profile

The utorque acceleration which is a four-step acceleration profile shown in figures 3.2(a) and (b) and the corresponding capsubot movement for this profile is shown in figures 3.3(a) and (b).For the utorque profile in step the inner mass and the capsubot move in the same direction as it is shown in figure 3.4(b) and in the opposite direction for steps 3 and 4. The inner mass moves in the forward direction for step 1 and 2 and in the backward direction for steps 3and 4 and the capsubot moves in the forward direction for the inner mass bidirectional movements .

The contrarium profile

The contrarium profile is a two-step acceleration profile which shown in figures 3.2(c) and 3.2(d) , for the contrarium profile the capsubot movement is in the opposite direction for the inner mass as it is shown in figures 3.5(b) and the inner mass only moves forward.

1.12.2 Motion generation

The four possible scenarios for motion generation are shown in figures 3.3(a) to 3.3(d) and based on the proposed accelerations profiles proposed by (Huda and Yu, 2015) an explanation is also given for two possible scenarios for figure 3.3(a) and 3.3(c) and the other two scenarios whose are figure 3.3(b) and 3.3(d) have similar principle respectively.

Scenario of figure 3.3(a) for the Utorque acceleration profile

Initially the inner mass is at the left end ($x_{IM} - x_M = -k$) and in the beginning of the cycle and the inner mass follows the acceleration shown in figure 3.2(a) and k is half length of the inner mass relative displacement and for this acceleration profile the inner mass moves from the left end to the right end and then it returns to the left end .The inner mass accelerations , velocities and displacements is shown in figure 3.4(a) to 3.4(c).

In step one the inner moves in the forward direction slowly with small positive acceleration and because of the friction is higher than the reaction force it dominated and capsubot does not move. In step two the inner mass moves forward with a big negative acceleration and the capsubot moves in forward direction with a positive acceleration and inner mass reaches the right end at this step and stops .In step three the capsubot has initial positive velocity and on this step the inner mass moves in the backward direction with a big negative acceleration and the capsubot receives a reaction the forward and moves forward due to the received force in the forward direction with a positive acceleration and the capsubot velocity higher than step two on this step . in the final step which is step four , the inner mass continue moving backward but with small positive acceleration and the capsubot moves in the forward direction with small positive acceleration for part of this step before it stops and it remain stationary as the friction is higher than the reaction force and the inner mass reaches to its left end and it stops more explanation is given in (Huda and Yu, 2015).

Scenario of figure 3.3(c) for the contrarium acceleration profile

At the beginning of the cycle the inner mass is at its left end $(x_{IM} - x_M = -k)$ and it follows the acceleration profile illustrated in figure 3.3(c) and in this acceleration profile the inner mass moves from the right end to the left end , therefore the accelerations , velocities and displacements for the inner mass and capsubot in various steps are in figures 3.5(a) to 3.5(c) and the contrarium profile is a two-step acceleration profile .

The steps are as following, in first step which is step one , the inner mass moves in the backward direction with big negative acceleration and at this stage a force is received , therefore the reaction force is greater than the friction ,thus the capsubot moves in forward direction with a positive acceleration.

in step two the inner mass continues to move backward with small positive acceleration and the capsubot in the other hand moves forward with small negative acceleration for a part of this step before it stops and remain stationary.

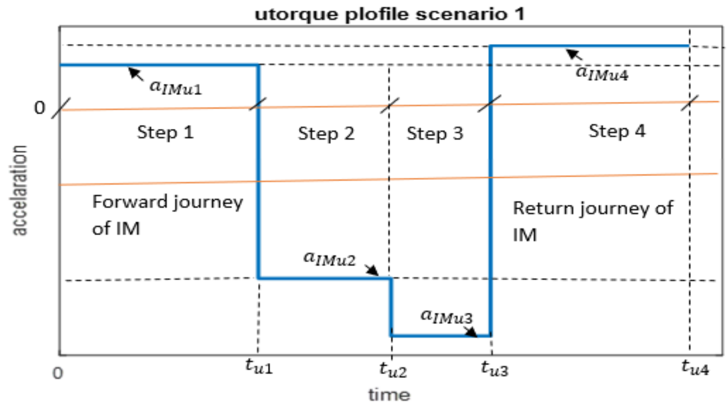

(a)The utorque profile scenario one (a_{IMu1},a_{IMu2},a_{IMu3} and a_{IMu4}) are the
inner mass accelerations in the four steps respectively and (t_{u1},t_{u2},t_{u3} and t_{u4}) are the time after each step respectively.

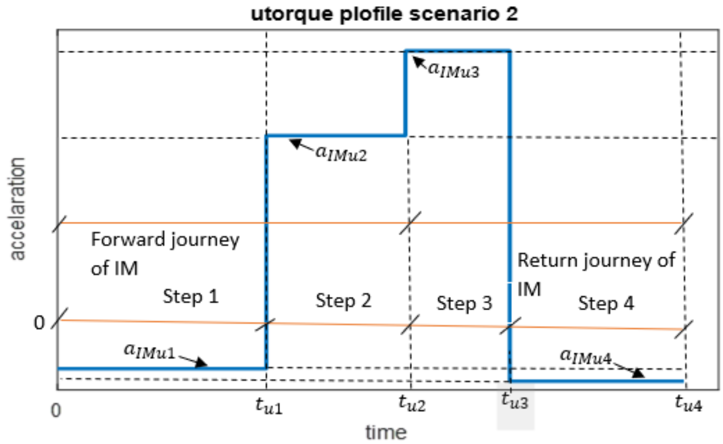

(b)The utorque profile scenario two (a_{IMu1},a_{IMu2},a_{IMu3} and a_{IMu4}) are the

inner mass accelerations in the four steps respectively and (t_{u1},t_{u2},t_{u3} and t_{u4})

are the time after each step

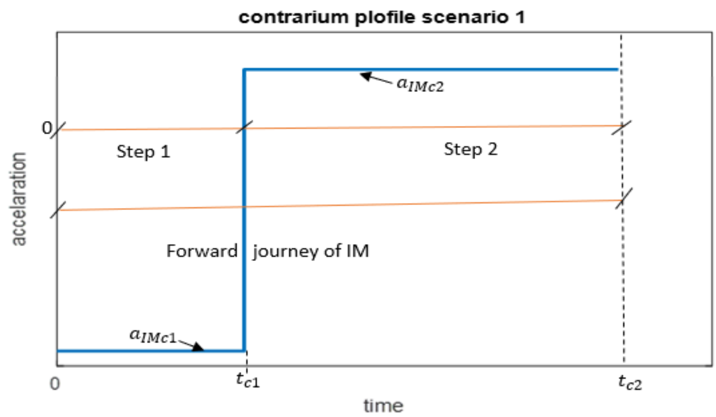

(c) the first scenario of contrarian profile a_{IMc1} and a_{IMc2} are the inner mass accelerations
for each step respectively and t_{c1} and t_{c2} are the time after each step

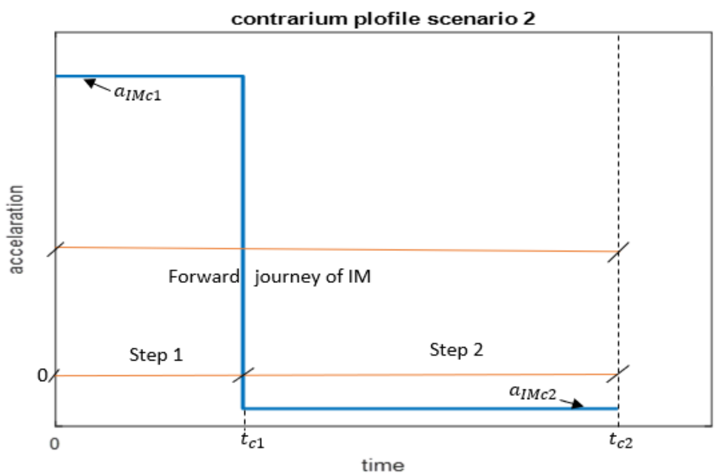

(d) the second scenario of contrarian profile a_{IMc1} and a_{IMc2} are the inner mass accelerations
for each step respectively and t_{c1} and t_{c2} are the time after each step

Figure 0.2: acceleration profiles for the inner mass

(Huda and Yu, 2015).

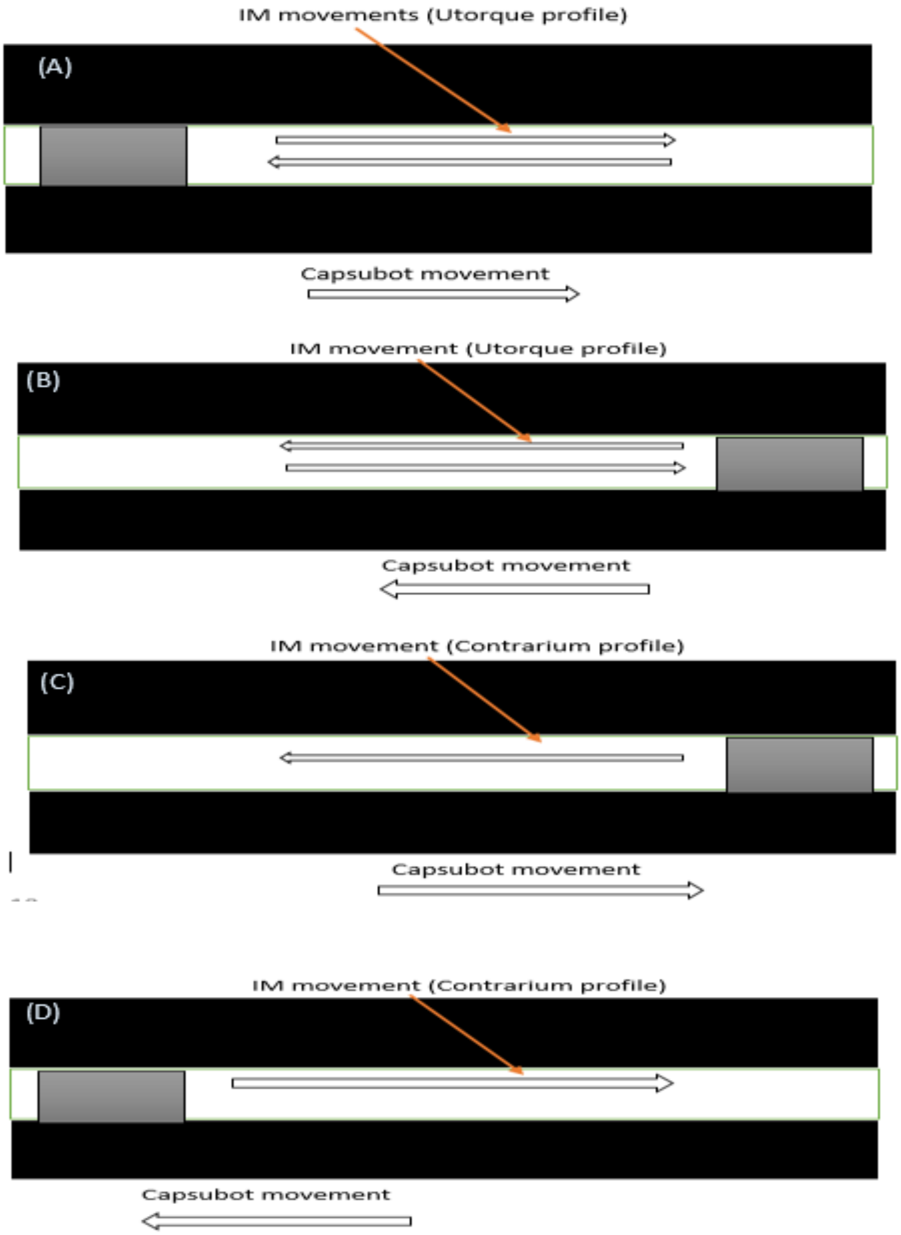

Figure 0.3 Capsubot possible scenarios for motion generation

In figure 3.3(a) as it is shown the inner mass is at the left end and the capsubot is moved to the right applying the utorque profile in 3.3(b) the inner mass the right end and capsubot been moved to the left applying utorque profile.

In figure 3.3(c) the inner mass is at the right end and the capsubot has been moved to the right applying the contrarium profile shown in figure 3.3(c) and after one cycle the inner mass reaches to the left end , therefore , it is ready to use the utroque profile shown in figure 3.3(a).

In the scenario 3.3 which is (d), initially the inner mass is at the left end and the capsubot has been moved to the left using the contrarium profile described by figure 3.3(d) and after one cycle the inner reaches right end and therefore is ready to use the utorque profile described by 3.3(b).

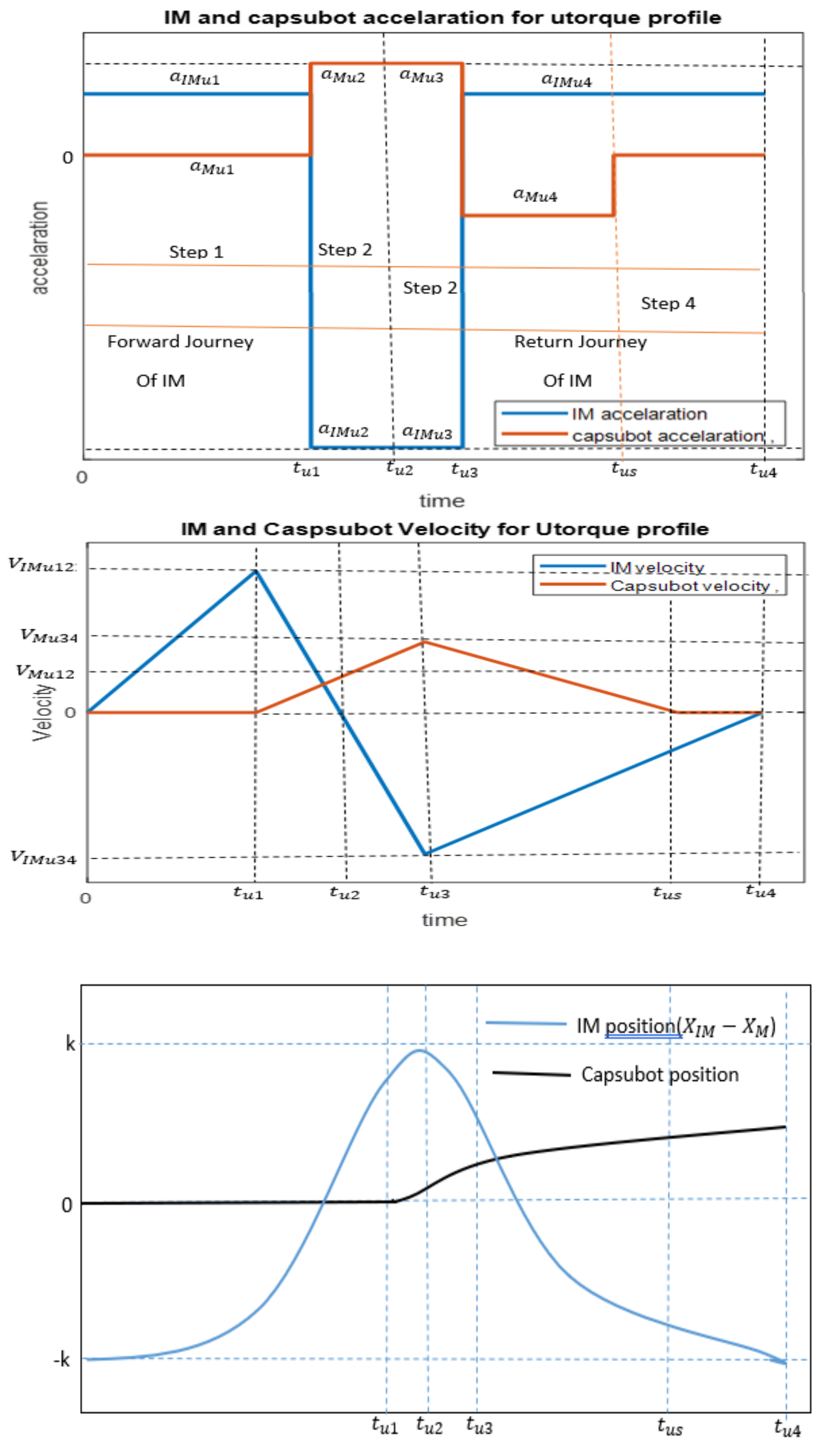

(a) Inner mass and capsubot accelerations

(b) Inner mass and capsubot velocities

(c) Inner mass and capsubot displacements

Figure 0.4 : Scenarios figures 3.2(a) and 3.3(a) acceleration velocities and positions for inner mass and capsubot for the utorque profile

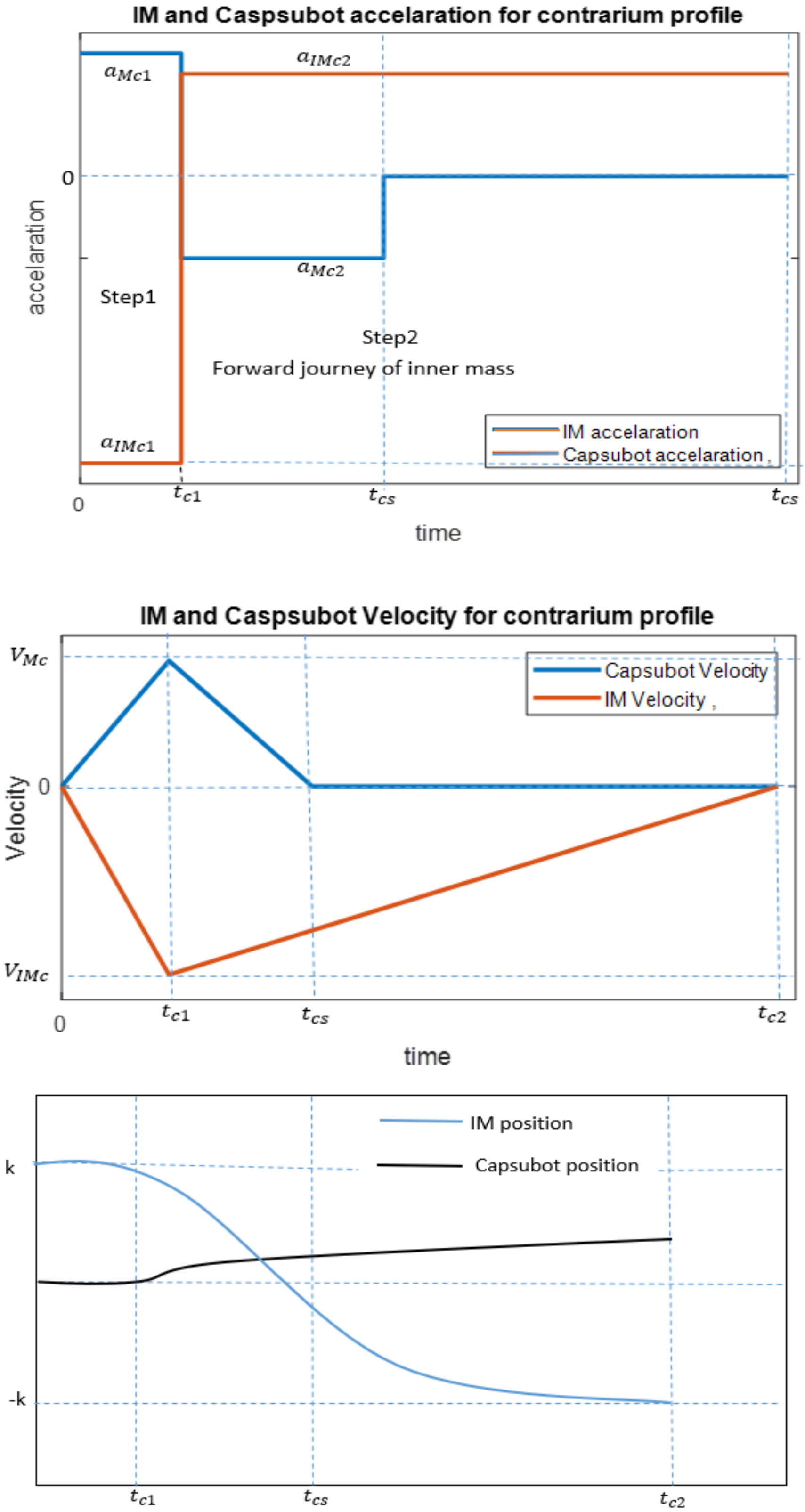

(a) Inner mass and capsubot accelerations

(b) Inner mass and capsubot velocities

(c) Inner mass and capsubot positions

Figure 0.5: Scenarios figures 3.2(c) and 3.3(c) acceleration velocities and positions for inner mass and capsubot for the contrarium profile

1.13 Selection of parameters for the acceleration profiles

1.13.1 Selection of parameters for the utorque profile

The optimum selection of acceleration profile parameters is given by (Huda and Yu, 2015). For the utorque can be as following from figure3.4(a) and 3.4(b).

$$\boldsymbol{t_{u1}} = \frac{|\boldsymbol{v_{IMu12}}|}{|\boldsymbol{a_{IMu1}}|} \;\; ; \;\; \boldsymbol{t_{u2}} = \boldsymbol{t_{u1}} + \frac{|\boldsymbol{v_{IMu12}}|}{|\boldsymbol{a_{IMu2}}|} \quad (3.48)$$

$$\boldsymbol{t_{u3}} = \boldsymbol{t_{u2}} + \frac{|\boldsymbol{v_{IMu34}}|}{|\boldsymbol{a_{IMu3}}|} \quad ; \boldsymbol{t_{u4}} = \boldsymbol{t_{u3}} + \frac{|\boldsymbol{v_{IMu34}}|}{|\boldsymbol{a_{IMu4}}|} \quad (3.49)$$

$$\boldsymbol{t_{us}} = \boldsymbol{t_{u3}} + \frac{|\boldsymbol{v_{M34}}|}{|\boldsymbol{a_{Mu3}}|} \quad (3.50)$$

$$\boldsymbol{v_{IMu12}} = \sqrt{\frac{4k a_{IMu1} a^2_{IMu2}}{a^2_{IMu2} - a_{IMu1}\, a_{IMu2} - a_{IMu1}\, a_{Mu2}}} \quad (3.51)$$

$$\boldsymbol{a_{Mui}} = \frac{-m a_{IMui-\mu_M M g}}{M} \quad \boldsymbol{i = 2, 3, 4} \quad (3.52)$$

$$\boldsymbol{v_{Mu12}} = -\frac{a_{Mu2}}{a_{IMu2}} \boldsymbol{v_{IMu12}} \quad (3.53)$$

$$\boldsymbol{v_{Mu34}} = -\frac{a_{Mu3}}{a_{IMu3}} \boldsymbol{v_{IMu34}} + \boldsymbol{v_{Mu12}} \quad (3.54)$$

And v_{IMu34} can be determined by solving the quadratic equation of v_{IMu34} .

$$\left(\frac{1}{a_{IMu3}} - \frac{1}{a_{IMu4}} + \left(\frac{1}{a_{Mu4}} - \frac{1}{a_{Mu3}}\right)\frac{{a_{Mu3}}^2}{{a_{IMu3}}^2}\right) v^2_{IMu34} + 2v_{IMu12}\frac{a_{Mu3}a_{Mu2}}{a_{IMu3}a_{IMu2}}\left(\frac{1}{a_{Mu4}} - \frac{1}{a_{Mu3}}\right) v_{IMu34} + \left(4k + \frac{v^2_{Mu12}a^2_{Mu2}}{a_{Mu4}a^2_{IMu2}} v^2_{IMu12}\right) = 0 \quad (3.55)$$

IM indicates inner mass and M indicates capsubot

1.13.2 Selection of parameters for the Contrarium profile from fig 3.5(a) and 3.5(b)

$$\boldsymbol{t_{C1}} = \frac{|v_{IMC}|}{|a_{IMc1}|} \;\; ; \;\; \boldsymbol{t_{c2}} = \boldsymbol{t_{c1}} + \frac{|v_{IMc}|}{|a_{IMc2}|} \tag{3.56}$$

$$\boldsymbol{t_{cs}} = \boldsymbol{t_{c1}} + \frac{|v_{Mc}|}{|a_{Mc2}|} \tag{3.57}$$

Where

$$\boldsymbol{v_{Mc}} = \frac{\boldsymbol{a_{Mc1}}}{\boldsymbol{a_{IMc1}}}\boldsymbol{v_{IMc}} \tag{3.58}$$

$$v_{IMc} = -\sqrt{\frac{-4ka_{IMc1}^{2}a_{IMc2}a_{Mc2}}{a_{IMc1}a_{Mc2}P - a_{Mc1}a_{IMc2}Q}} \tag{3.59}$$

for 3.45 P = a_{IMc2}-a_{IMc1} and Q=$a_{Mc1} - a_{Mc1}$ and to calculate $a_{Mc1}$and a_{Mc2} the equation below can be used

$$a_{Mci} = \frac{-ma_{IMci} - \mu_M Mg}{M}; i = 1,2. \tag{3.60}$$

(Huda and Yu, 2015)

Chapter Four

1.14 Control

In order to track the given trajectory of the capsubot position, the control approach proposed by (Huda and Yu, 2015) is used, which is a two-stage control approach shown in figure (4.1). The capsubot mechanical property is underactuated machinal system, which makes its control challenging, due to the degree of freedom needs to be controlled which is greater than the control input, therefore the control input is divided into two stages in (Huda and Yu, 2015) as it described below in figure(4.1),in order the two-stage control approach the following step will be followed as it was proposed .

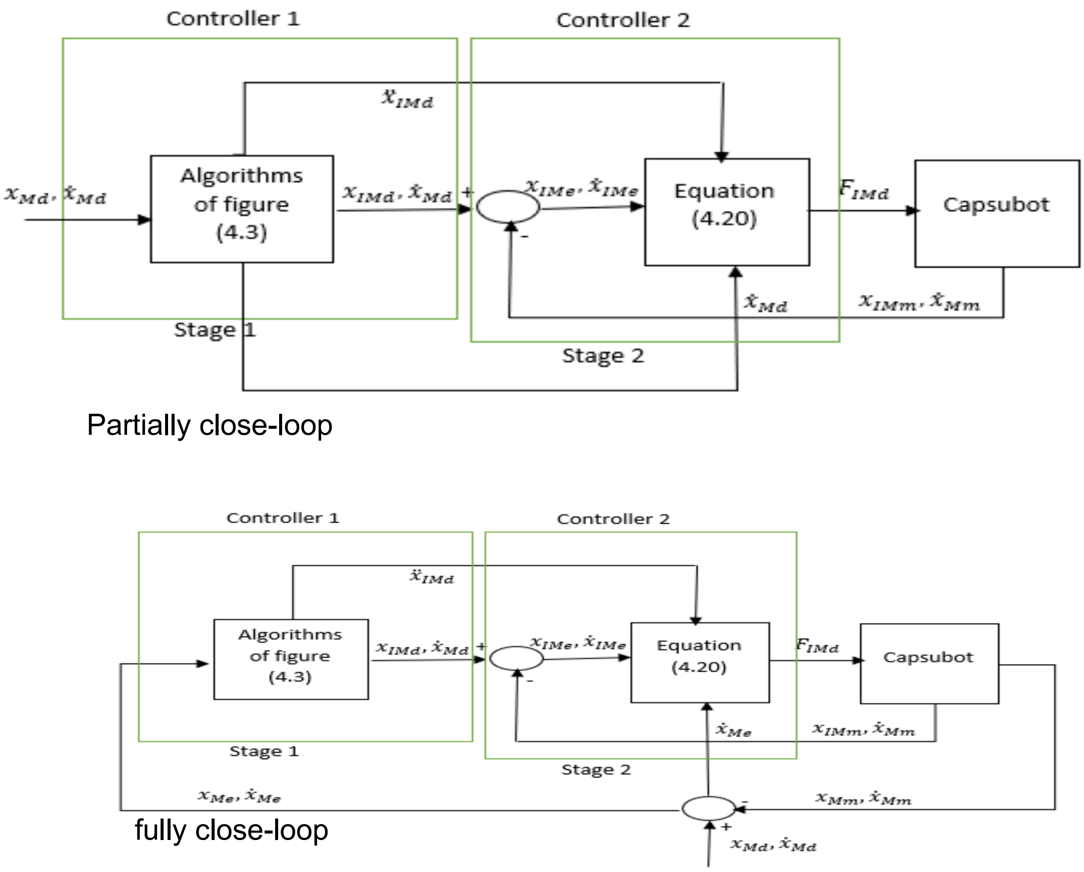

Figure 0.1 capsubot control system schematic

The proposed two stage control strategy by (Huda and Yu, 2015) for open loop control modified above in figure (4.1) to close-loop control system. To obtain the close-loop control , the capsubot displacement and velocity can be tracked using sensor such as (inertia measurement unit) and the measured capsubot velocity and displacement can be added to the desired and the error can be feedback to the system to correct the system input as it is shown in the figure above. For this research the system was considered partially close-loop ,which means the inner mass system was close-loop but the capsubot was open-loop.

1.14.1 Database creation

For the purpose of tracking the capsubot trajectory, there will be a requirement for the capsubot average velocities for different inner mass acceleration. The average velocity is given as following and it is shown in figure 3.4(c) .

$$\bar{\dot{x}}_{Mu} = \frac{x_{Mu}}{t_u} \tag{4.1}$$

x_{Mu} indicates the capsubot displacement in time cycle t_u in the utorque profile.

$$x_{Mu} = \frac{v_{Mu12}^2}{2a_{Mu2}} + \frac{v_{Mu34}^2 - v_{Mu12}^2}{2a_{Mu3}} - \frac{v_{Mu34}^2}{2a_{Mu4}} \tag{4.2}$$

$$t_u = t_{u4} = \frac{|v_{IMu12}|}{|a_{IMu1}|} + \frac{|v_{IMu12}|}{|a_{IMu2}|} + \frac{|v_{IMu34}|}{|a_{IMu3}|} + \frac{|v_{IMu34}|}{|a_{IMu4}|} \tag{4.3}$$

The capsubot average velocities for the contrarium profile from figure 3-5(c) is given by

$$\bar{\dot{x}}_{Mc} = \frac{x_{Mc}}{t_c} \tag{4.4}$$

x_{Mc} indicates the capsubot displacement in time cycle t_c in the conrarium profile.

$$x_{Mc} = \frac{v_{Mc}^2}{2a_{Mc2}} - \frac{v_{Mc}^2}{2a_{Mc2}} \tag{4.5}$$

$$t_u = t_{u4} = \frac{|v_{IMc}|}{|a_{IMc1}|} + \frac{|v_{IMc}|}{|a_{IMc2}|} \tag{4.6}$$

The capsubot average velocity for the contrarium profile from fig3.5(c) is

$$\bar{x}_{Mc} = \frac{x_{Mc}}{t_c} \tag{4.7}$$

Thus x_{Mc} is the capsubot displacement in cycle time t_c in the contrarium profile

Where

$$x_{Mc} = \frac{v_{Mc}^2}{2a_{Mc1}} - \frac{v_{Mc}^2}{2a_{Mc2}} \tag{4.8}$$

$$t_c = t_{c2} = \frac{|v_{IMc}|}{|a_{IMc1}|} + \frac{|v_{IMc}|}{|a_{IMc2}|} \tag{4.9}$$

$$n_u = floor(\frac{|a_{IMumax}| - |a_{IMumin}|}{a_{IMudiff}} + 1 \tag{4.10}$$

$$n_c = floor(\frac{|a_{IMcmax}| - |a_{IMcmin}|}{a_{IMcdiff}} + 1 \tag{4.11}$$

(Huda and Yu, 2015)

1.14.2 Inner Mass and capsubot desired trajectory generation

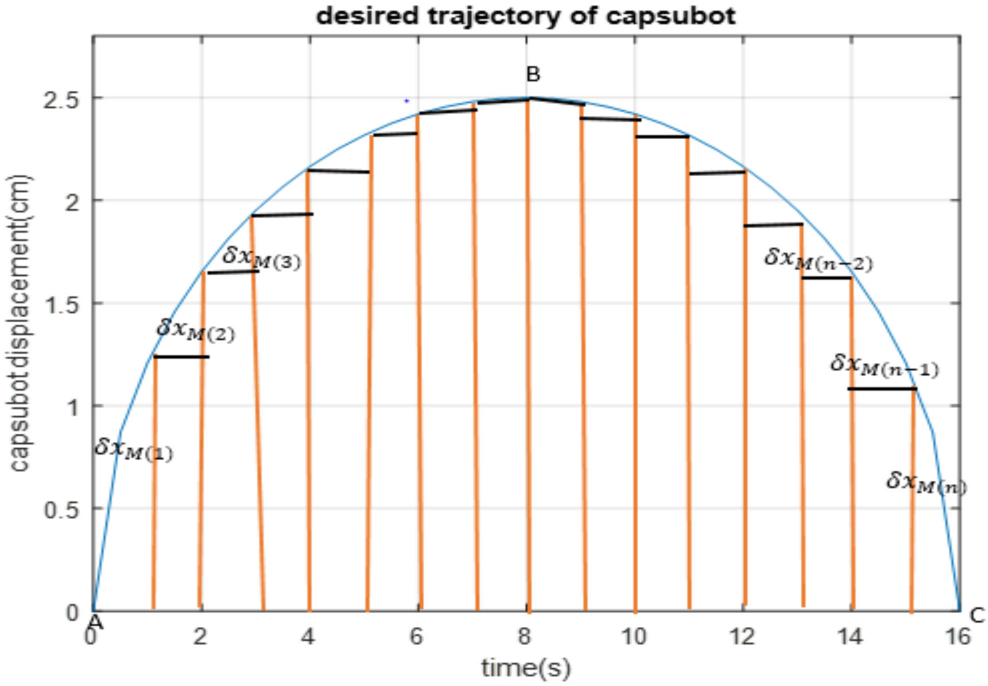

Figure 0.2:1D desired trajectory tracking generation for inner mass (segment-wise)

Due to the dynamic of the capsubot which is underactuated mechanical the capsubot cannot be controlled directly and can be controlled indirectly by controlling the movement of the inner mass. Based on the desired trajectory a segment can be designed .T is the time of each segment, $\delta x_{M(i)}$ is the required displacement in ith segment and the desired average velocity is given by equation (4.12), (Huda and Yu, 2015), using the guideline given by (Huda, 2019), the close-loop control for the system can implemented by replacing equation(4.12) by equation(4.13).

$$\bar{\dot{x}}_{Md(i)}=\frac{\delta x_{M(i)}}{T} \tag{4.12}$$

$$\bar{\dot{x}}_{Md(i)}=\frac{\delta x_{M(i)+x_{Mm(i-1)}}}{T} \tag{4.13}$$

$$x_{Mme(i)}=x_{Md(i)}-x_{Mm(i)} \tag{4.14}$$

x_{Md} is the capsubot desired position and x_{Mm} is the capsubot measured position, $\bar{\dot{x}}_{Md}$ capsubot desired average velocity.

1.14.3 Selection algorithms

The capsubot average velocity is compared with the database created in section 4.1.1 for each sech segment of 1d capsule robot (capsubot) trajectory and to do so the following two steps needs to be followed

Step 1 .an acceleration profile needs to be selected, normally one of the two utorque profiles is selected and the four possible acceleration profiles are described by fig (3.2), 3.2(a) is selected for positive average capsubot velocity and 3.2(b) for negative average capsubot velocity, in the case when switching between the utorque profile is required ,for example the inner mass returns to its initial position after each cycle and for the switching one of the contrarium profiles is used ,whose are described by fig 3.2(c) and 3.2(d)

Step 2. To generate the required average velocity ,two parameters needs to be selected for the utorque profile , a comparison will be performed between the desired average velocity between and the projected average velocity and the profile set that corresponds to minimum error is selected ,for more detailed explanation please see (Huda and Yu, 2015).

$$\dot{x}_{diff} = \min\Big((|\bar{\dot{x}}_{Md} - \bar{\dot{x}}_{Mu}(1)|), (|\bar{\dot{x}}_{Md} - \bar{\dot{x}}_{Mu}(2)|), \dots \dots, (|\bar{\dot{x}}_{Md} - \bar{\dot{x}}_{Mu}(n_u)|)\Big) \quad (4.15)$$

$$\dot{x}_{diff} = \min\Big((|\bar{\dot{x}}_{Md} - \bar{\dot{x}}_{Mu}(1)|), (|\bar{\dot{x}}_{Md} - \bar{\dot{x}}_{Mu}(2)|), \dots \dots, (|\bar{\dot{x}}_{Md} - \bar{\dot{x}}_{Mu}(n_u)|)\Big) \quad (4.16)$$

Step 3 is about tuning the segment time, in order to operate the acceleration profile for a multiple cycle of time and the selected parameter will be applied for the time period.

$$T_{tuned} = t_{selec} \times floor(\frac{T}{t_{selec}}) \quad (4.17)$$

1.14.4 Control of the Inner mass

The open control law of the Inner mass with coulombs friction model is

$$F_{IMd} = \mathrm{m}\ddot{x}_{md} + sgn(\dot{x}_{IMd} - \dot{x}_{capd})\mu_{IM}mg \quad (4.18)$$

And the open law control for the inner mass with LuGree friction is

$$F_{IMd} = m\ddot{x}_{IMd} + \sigma_{0IM}Z_{IM} + \sigma_{1IM}\dot{Z}_{IM} + \sigma_{2IM}(\dot{x}_{IMd} - \dot{x}_{capd}) \quad (4.19)$$

And the close-loop control law can be selected using the partial feedback linearization (Yu et al. 2008)

$$F_{IMd} = \alpha\tau_{md} + \beta \quad (4.20)$$

Where $\alpha = m$ and $\beta = sgn(\dot{x}_{IMd} - \dot{x}_{capd})\mu_{IM}mg$ for 4.18 and $\beta = \sigma_{0IM}Z_{IM} + \sigma_{1IM}\dot{Z}_{IM} + \sigma_{2IM}(\dot{x}_{IMd} - \dot{x}_{capd})$ for (4.19) ,and the tracking error $\tilde{x}_m = x_{me} = x_{IMm} - x_{IMd}$ and choosing the linear control law

$$\tau_{md} = \ddot{x}_{IM} - k_1\dot{\tilde{x}}_{IM} - k_2\tilde{x}_{IM} = 0 \quad (4.21)$$

k_1 *and* k_2 can be selected using the standard linear control theory and by using (4.20) we can the inner mass follow the desired trajectory (Huda and Yu, 2015).

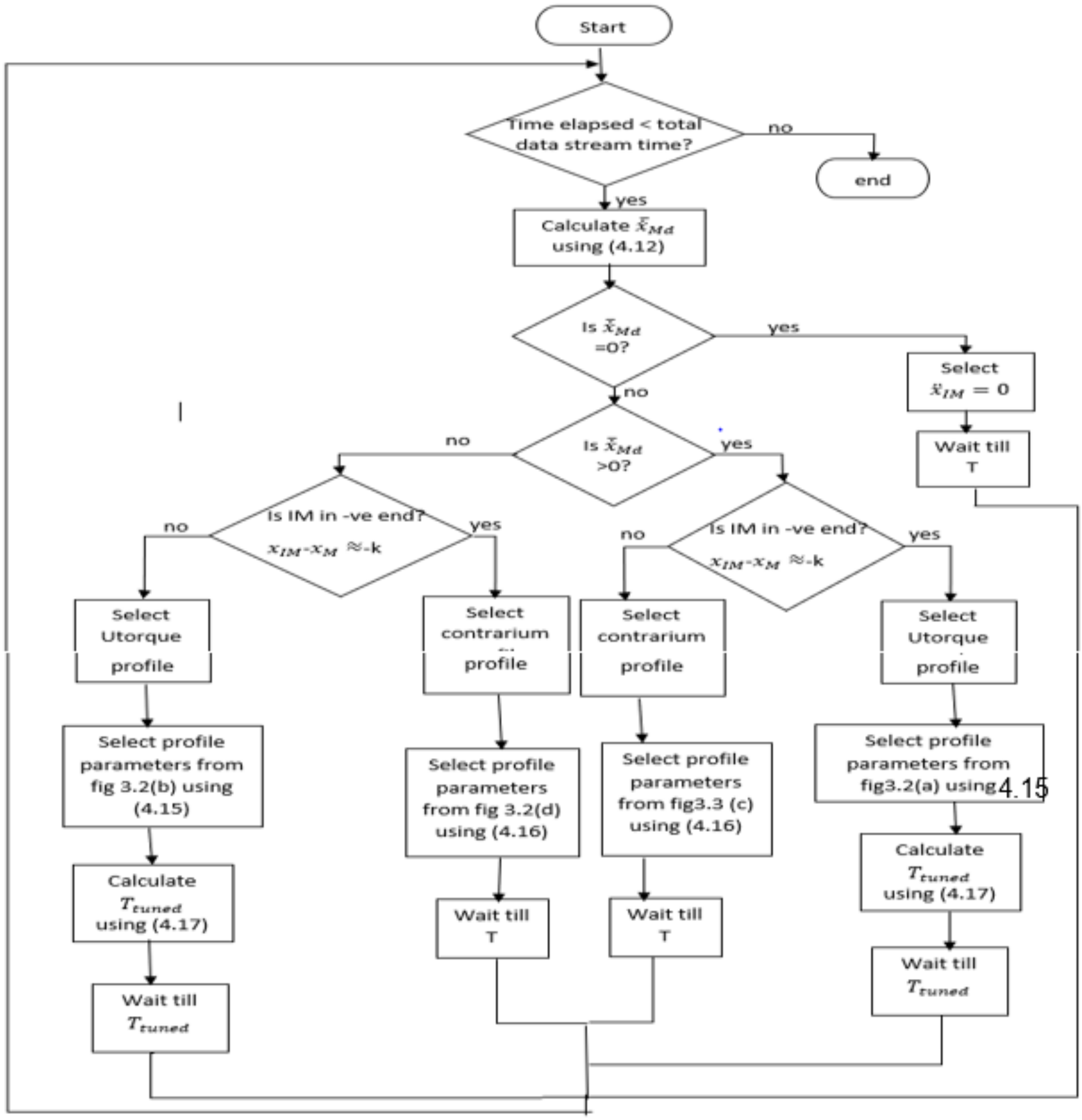

Figure 0.3: selection algorithms flowchart

Chapter Five Testing and Results

1.15 Simulation setup and results discussion

Each part of the model was simulated in MATLAB and Simulink and the analysis of the performance was also conducted in the same environment , the simulation is with two friction models , the first model is the system with coulombs friction model ,which means the capsubot and the inner mass was modelled with coulombs friction model and the parameters for this model is shown in table(5.1) and the Simulink models are shown appendix (A).

The second model is the model, modelled with LuGree friction , the parameters for this friction model is more complex than the coulombs friction ,however an initial assumption was made for parameters to conduct the simulation analysis and the assumed values are small as it is shown in table (5.2).

M	0.396 kg
m	0.05 kg
μ_M	0.1
μ_m	0.2
k	9mm

Table 0.1:parameters for 1D capsubot with coulombs friction model

M	0.396 kg
m	0.05 kg
μ_M	0.1
μ_m	0.2
k	9mm
$sig0_{IM}$ (stiffness of material relevant to Inner mass)	0.3
$sig1_{IM}$(material damping coefficient relevant to Inner mass)	0.1
$sig2_{IM}$ (viscous damping coefficient relevant to Inner mass)	0.2
$sig0_{cap}$(stiffness of material relevant to Inner mass)	0.3
$sig1_{cap}$ (material damping coefficient relevant to capsubot)	0.3
$sig2_{cap}$ (viscous damping coefficient relevant to capsubot)	0.2
f_{s_cap} (capsubot static friction)	0.47
f_{s_IM} (Inner mass static friction)	0.3
fv_{cap} (capsubot stribeck velocity)	0.1
fv_{IM} (Inner mass stribeck velocity)	0.1
Z_{IM} (micro displacement or bristle deflection relevant to Inner mass)	0.1
Z_{cap} (micro displacement or bristle deflection relevant to capsubot)	0.001

Table 0.2:parameters for 1D capsubot with LuGree friction model

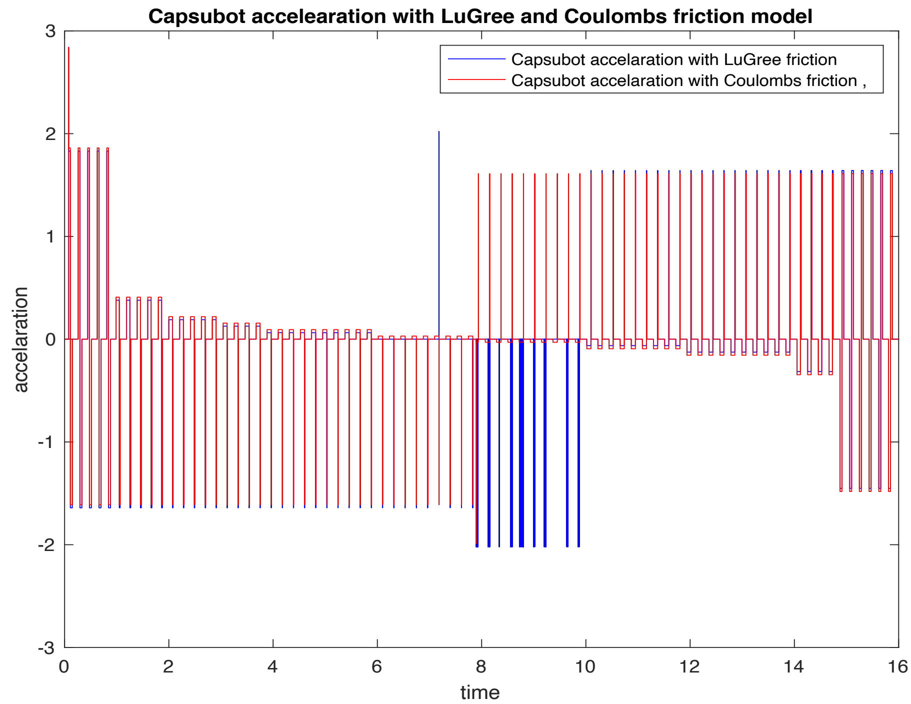

Figure 0.1: capsubot acceleration with coulombs friction model vs acceleration with LuGree friction model

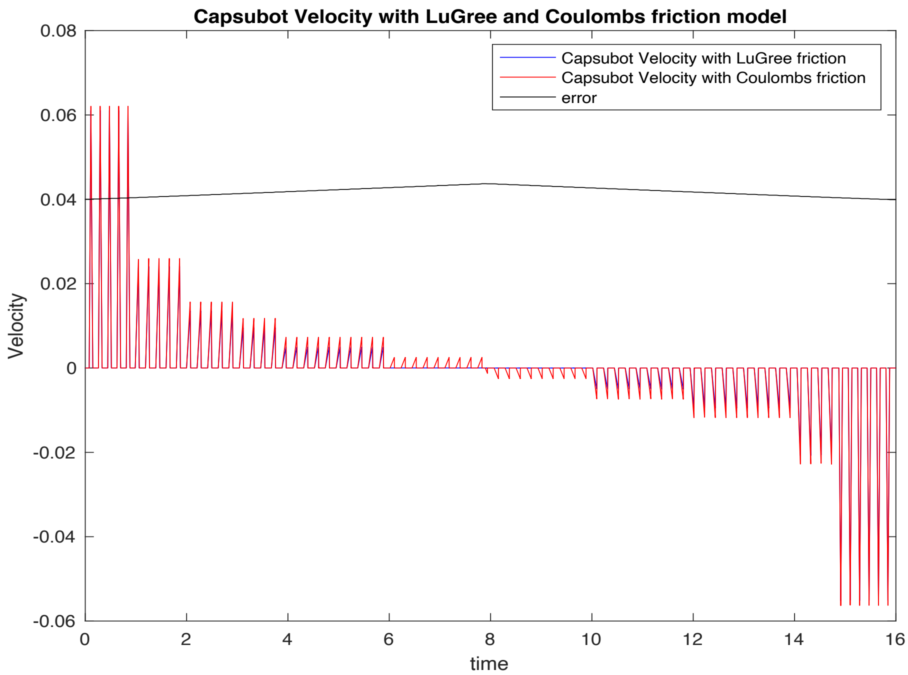

Figure 0.2:capsubot velocity with coulombs friction model and capsubot velocity with LuGree friction model

In Fig (5.1) we see the capsubot acceleration for both models ,the model with coulombs friction model and the model with LuGree friction model, for comparison purposes and similarly in Fig(5.2) the capsubot velocities for both cases ,the model with coulombs friction and the model with LuGree friction model.

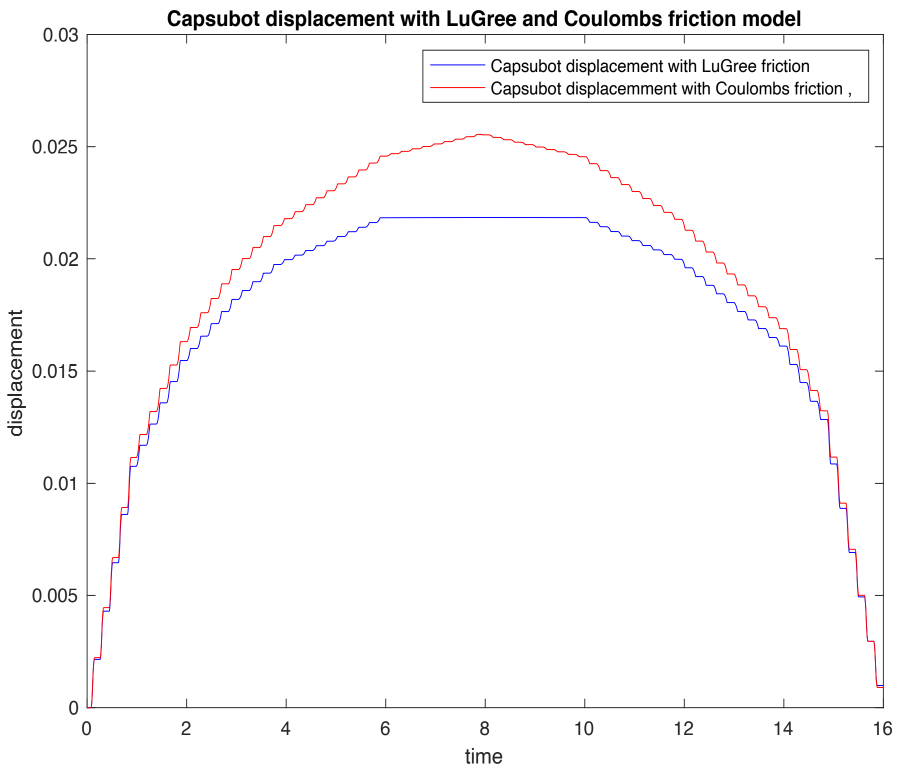

Figure 0.3:capsubot displacement with coulombs friction model and LuGree friction

Figure (5.3) shows the capsubot trajectory for both cases, the case with LuGree friction and the case with the coulombs friction for the purpose of comparison, from the figure above we observe that the capsubot moves from 0cm to 2.5cm in 8 seconds and returns to 0 cm again in 8 seconds ,this case is true for the model with coulombs friction but its slightly different for the model with LuGree friction model , with the LuGree friction we observe that the trajectory of the capsubot is as following ,the capsubot moves from 0cm to position 2.3 cm in 6 seconds and then carry on in the same position from 4 seconds after that returns to starting position in 6 seconds. And this can also be observed in Fig(5.2) the capsubot acceleration for both cases ,its observed that the capsubot accelerates for 2 more seconds instead of decelerating and start to decelerate .

The obtained results shows that the caspubot acceleration, velocity and displacement are slightly different and this could be due to the parameters ,despite the LuGree friction model describes most of the friction phenomena such as in pre-sliding , the stiction to crossing zero velocity but it is characterised by six parameters whose are the frictional damping , the frictional stiffness, the viscous coefficient, the coulombs friction , the static friction and the stribeck velocity and for the purpose of performing the simulation most of these parameters have been assumed .therefor using the correct parameters may result in a better output.

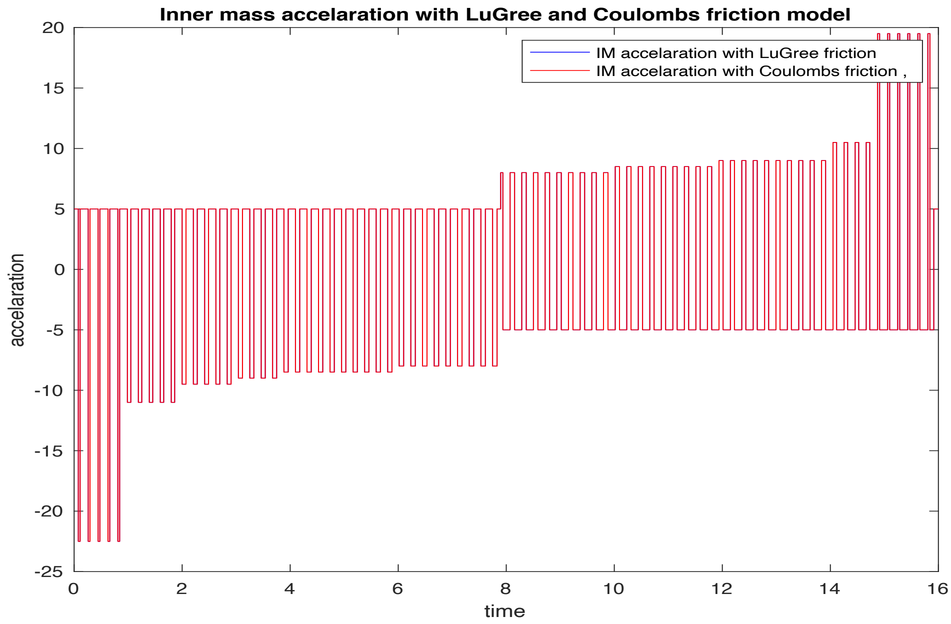

Figure 0.4:Inner mass acceleration with coulombs friction model and inner mass acceleration with LuGree friction

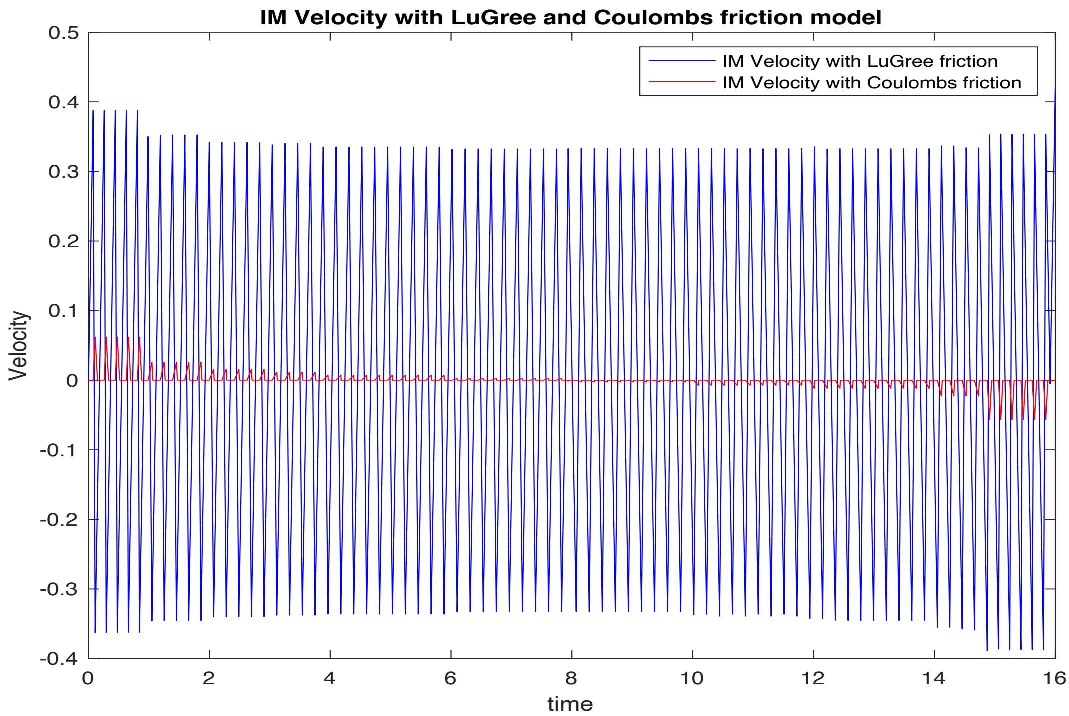

Figure 0.5:Inner mass velocity with coulombs friction model and inner mass velocity with LuGree friction

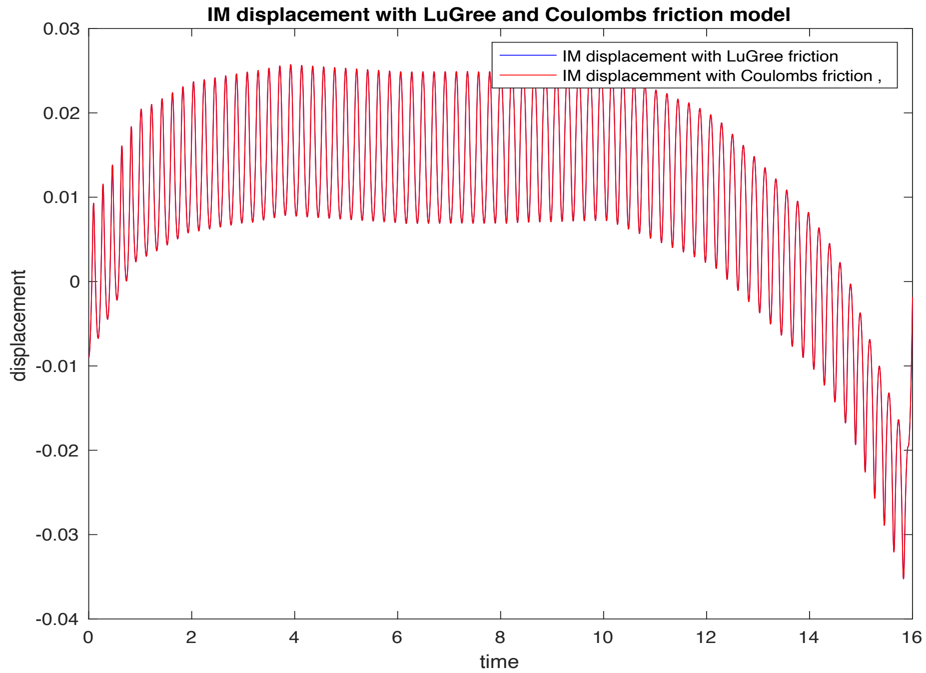

Figure 0.6:Inner mass displacement with coulombs friction model and inner mass displacement with LuGree friction

the capsubot follows the trajectory tracking control shown in fig(4.2) to track the desired trajectory which is the segment-wise tracking , for the coulombs model we observe that the capsubot moves with high positive velocity at the beginning and then the velocity decreases to get to zero at 8 seconds and then the 1D capsule robot (capsubot) moves with negative velocity and the magnitude of the velocity increases with time till the end of the trajectory and by the end of the trajectory reaches its maximum as it is shown in Fig(5.2).

As it is observed in Fig (5.2) the inner mass velocity for systems with both friction models, the system with coulombs friction model, we see that the inner mass starts with high positive velocity and then gradually decreases and it gets to zero when the time is 8 seconds and changes polarity and it keeps increasing till it gets to its maximum by the end of the trajectory .However, we observe that the case is different for the system modelled with LuGree friction model , we see that the inner velocity has higher magnitude and almost constant, from the beginning to the end of the trajectory.

As it is observed in the obtained results above , we see that the system modelled with coulombs friction is more closer to desired trajectory, however the disadvantages of this model does not capture the friction in various stages because its basic modelling .Therefore ,the LuGree friction model is the alternative and it does describe most of the friction phenomena and we observed that from the simulation results with assumed parameters ,the results almost the same.

1.16 Hardware setup and 3D design of capsubot

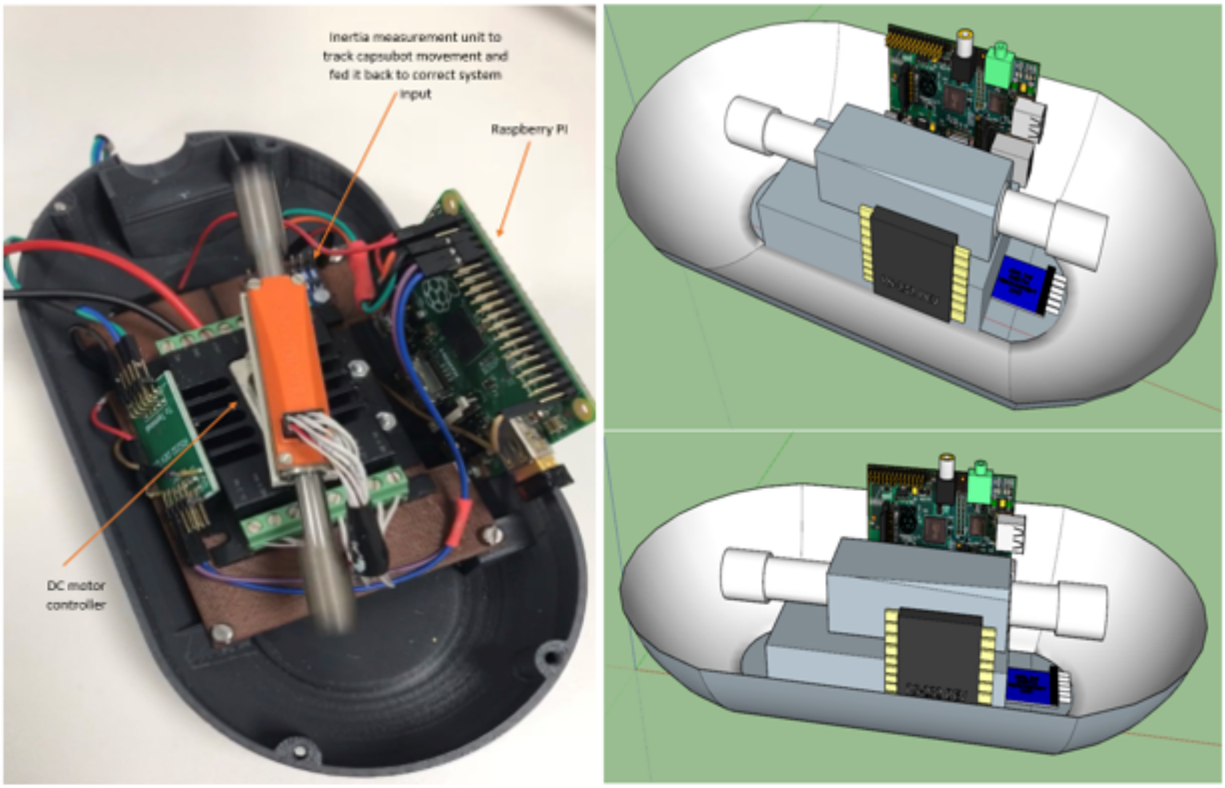

Figure 0.7: 1D capsule robot(capsubot) hardware and 3D design

To conduct hardware, experiment the capsubot can be developed as it shown in Fig (5.7), which is hardware implementation and conceptual 3D design of 1D capsule robot (capsubot). The component required to develop the capsubot are linear DC motor such as the (QUICKSHAFT LM1247-020-01), two batteries, motion controller and shell that holds the system components together. And to implement a close-loop system an inertia measurement unit is required. However, on this, thesis there's no hardware that was presented. The constrains shown in table (5.3) were used for the simulation and it can be used for any experiment work for this project in the future.

Stroke length of Inner mass	20mm
Maximum achievable continues acceleration of IM	$\pm 30\ ms^{-2}$
Maximum continues force of inner mass	3.09N
Peak force of inner mass	9.26N
I_{peak} continues of motor coil	0.48A
I_{peak} continues of motor coil	1.44A

Table 0.3: Simulation and Experiment constrains

Chapter Six

1.17 Conclusions

This research has performed the following objectives, the design, mathematical modelling, linearization and trajectory tracking control of underactuated mechanical system with different friction models and implemented the developed mathematical models in simulation environment MATLAB and Simulink.

This research mainly focused on developing new mathematical modelling with different friction models for 1D capsule robot (capsubot), which is a class of underactuated mechanical systems. Alongside the system model with coulombs friction, two other models with two different friction models has been proposed on this thesis, the two different models are a system mathematical model and its friction phenomena described by stribeck friction and the second model its friction is described by the LuGree friction model. The mathematical modelling for all three models is presented in chapter three. however, only two models have performance have been investigated on simulation environment the coulombs model and the LuGree model. A simulation has not been developed for the stribeck because the LuGree model can also describe the stribeck model.

The developed mathematical model with LuGree friction has many advantages for designing the capsubot for medical application ,engineering diagnosis or disaster rescue because the capsubot might be operating in environment with uncertainty and to capture the friction regime within such environment, a more advanced friction model is required such as the LuGree friction model.

This thesis also proposed a way to linearize the developed models which consist of scaler sgn function and the absolute function and this was achieved by replacing the mentioned non-smooth function by approximated equivalent function.

The obtained results from the simulation for the system modelled with the LuGree friction is slightly different from the system modelled with the coulombs such the inner velocity ,the capsubot displacement and the capsubot velocity and this due to the parametrisation of the LuGree friction ,in which all the parameters have been assumed but for the coulombs friction model all the parameters was obtained from real life experiment.

1.18 Achievements

The main goal of this thesis was to develop a new mathematical model for the capsubot system with more advanced friction model , a model that can describe the friction in a very advanced way and this was achieved by modelling both frictions within the system ,the inner mass friction and the friction between the shell and surface in motion with the LuGree friction model , the new model was simulated in MATLAB/Simulink and the performance was compared with a basic friction model, which the coulombs.

The second goal of the thesis was to linearize the system, and this was achieved mathematically and its presented in chapter three.

1.19 Recommendations for Future Work

In this thesis a new mathematical model for the system was proposed , the new model friction was described by the LuGree but the parameters has been estimated, to obtain a better intuition on how the model performs, a capsubot hardware needs to be developed so an experiment can be conducted with different environment uncertainty.

A linearized model was proposed a simulation can be developed for the linear model and it can be compared with nonlinear model, a different approach it can applied to control the linear model.

After developing the capsubot hardware, a fully close-loop control for the entire system can be achieved by adding a sensor such as the inertia measurement unit(IMU) and this will result to more accurate and reliable capsubot.

Student reflection

There are many invaluable skills that I have gained throughout this project such as project planning, time management, developing a new idea, research skills, mathematical modelling. This research enhanced my skills and gave me the opportunity to explore the field of robotics engineering, the main technical skills that I have improved throughout this project are applying mathematical skills to solve engineering problems and using simulation environment to test ideas such as MATALAB and Simulink.

This research also introduced me to the field of nonlinear control as well as linearization of nonlinear system and many other topics in robotics engineering.

Finally, I would like to say this project gave an invaluable skills as engineering student which will be very helpful in the real world such the project planning, time management ,presentation ,sharing ideas and mainly research skills.

Bibliography and References

1. Huda, M. and Yu, H. (2015). Trajectory tracking control of an underactuated capsubot. *Autonomous Robots*, 39(2), pp.183-198.

2. N. Lee, N. Kamamichi, H. Li and K. Furuta, "Control system design and experimental verification of Capsubot," *2008 IEEE/RSJ International Conference on Intelligent Robots and Systems*, Nice, 2008, pp. 1927-1932

3. Liu, Y., Yu, H. and Yang, T. (2008). Analysis and Control of a Capsubot. *IFAC Proceedings Volumes*, 41(2), pp.756-761.

4. Liu, Y., Yu, H. and Yang, T. (2008). Analysis and Control of a Capsubot. *IFAC Proceedings Volumes*, 41(2), pp.756-761.

5. Liu, Y., Pavlovskaia, E., Hendry, D. and Wiercigroch, M. (2013). Vibro-impact responses of capsule system with various friction models. *International Journal of Mechanical Sciences*, 72, pp.39-54.

6. Liu, P., Yu, H. and Cang, S. (2017). Geometric analysis-based trajectory planning and control for underactuated capsule systems with viscoelastic property. *Transactions of the Institute of Measurement and Control*, 40(7), pp.2416-2427.
7. Liu, Y., Yu, H. and Yang, T. (2008) "Analysis And Control Of A Capsubot". *IFAC Proceedings Volumes* [online] 41 (2), 756-761. available from <https://www.sciencedirect.com/science/article/pii/S1474667016390401> [12 October 2019]

8. Liu, P., Yu, H. and Cang, S. (2017) "Geometric Analysis-Based Trajectory Planning And Control For Underactuated Capsule Systems With Viscoelastic Property". *Transactions Of The Institute Of Measurement And Control* [online] 40 (7), 2416-2427. available from <https://journals.sagepub.com/doi/full/10.1177/0142331217708833> [20 October 2019]
9. Tuan, L. and Lee, S. (2016). Dynamic Modelling and Simulation of an Underactuated System. *IOPscience*, [online] 850(10.5772/64739). Available at

10. Liu, P., Yu, H. and Cang, S. (2017) "Geometric Analysis-Based Trajectory Planning and Control For Underactuated Capsule Systems with Viscoelastic Property". *Transactions Of The Institute Of Measurement And Control* [online] 40 (7), 2416-2427. available from <https://journals.sagepub.com/doi/full/10.1177/0142331217708833> [20 October 2019]

11. Liu, P., Yu, H. and Cang, S. (2018) "Optimized Adaptive Tracking Control For An Underactuated Vibro-Driven Capsule System". *Nonlinear Dynamics* [online] 94 (3), 1803-1817. available from <https://link.springer.com/article/10.1007/s11071-018-4458-9> [24 October 2019]
12. Farahani, A., Suratgar, A. and Talebi, H. (2013). Optimal Controller Design of Legless Piezo Capsubot Movement. *International Journal of Advanced Robotic Systems*, [online] 10(2), p.126. Available at: https://www.researchgate.net/publication/276184104_Optimal_Controller_Design_of_Legless_Piezo_Capsubot_Movement [Accessed 24 Oct. 2019].
13. Liu, P., Yu, H. and Cang, S. (2019). Modelling and analysis of dynamic frictional interactions of vibro-driven capsule systems with viscoelastic property. *European Journal of Mechanics - A/Solids*, [online] 74, pp.16-25. Available at: https://www.sciencedirect.com/science/article/pii/S0997753818301177 [Accessed 25 Oct. 2019].
14. Huda, N. (2019). *Bournemouth University Research Online [BURO] - Design, analysis and trajectory tracking control of underactuated mobile capsule robots.*. [online] Eprints.bournemouth.ac.uk. Available at: http://eprints.bournemouth.ac.uk/24994/ [Accessed 14 Oct. 2019].
15. Rentschler, M., Platt, S., Dumpert, J., Farritor, S. and Oleynikov, D. (2006). In vivo laparoscopic robotics. *International Journal of Surgery*, [online] 4(3), pp.167-171. Available at: https://www.sciencedirect.com/science/article/pii/S1743919106000781 [Accessed 9 Oct. 2019].
16. Li, Z. and Chiu, P. (2018). Robotic Endoscopy. *Visceral Medicine*, [online] 34(1), pp.45-51. Available at: https://www.karger.com/Article/Fulltext/486121 [Accessed 15 Oct. 2019].
17. Okamura, A., Chritensen, H. and J.Mataric, M. (2010) *Medical And Healthcare Robotics* [online] available from <https://www.researchgate.net/publication/252059583_Medical_and_HealthCare_Robotics> [12 October 2019]
18. Marcus, H., Nandi, D., Darzi, A. and Guang-Zhong Yang (2013) "Surgical Robotics Through A Keyhole: From Today's Translational Barriers To Tomorrow's “Disappearing” Robots". *IEEE Transactions On Biomedical Engineering* [online] 60 (3), 674-681. available from <https://ieeexplore.ieee.org/document/6423827> [5 November 2019]
19. Okamura, A., Chritensen, H. and J.Mataric, M. (2010) *Medical And Healthcare Robotics* [online] available from <https://www.researchgate.net/publication/252059583_Medical_and_HealthCare_Robotics> [12 October 2019]
20. NA, N. (2019). *LM1247-020-01 Linear Brushless DC Motor | MICROMO*. [online] Micromo.com. Available at: https://www.micromo.com/lm1247-020-01.html [Accessed 5 Nov. 2019].
21. Olsson, H., Åström, K., Canudas de Wit, C., Gäfvert, M. and Lischinsky, P. (1998). Friction Models and Friction Compensation. *European Journal of Control*, 4(3), pp.176-195.
22. Nnaji, A. (2017). *Modelling and Control of Position and Velocity Drives Subject to Friction*. Ph.D thesis. University of Reading.

23. Wojewoda, J., Stefański, A., Wiercigroch, M. and Kapitaniak, T. (2007). Hysteretic effects of dry friction: modelling and experimental studies. *Philosophical Transactions of the Royal Society A: Mathematical, Physical and Engineering Sciences*, [online] 366(1866), pp.747-765. Available at: https://royalsocietypublishing.org/doi/full/10.1098/rsta.2007.2125 [Accessed 13 Feb. 2020].

24. "I. On The Theory Of Lubrication And Its Application To Mr. Beauchamp Tower'S Experiments, Including An Experimental Determination Of The Viscosity Of Olive Oil" (1886) [online] 40 (242-245), 191-203. available from <https://royalsocietypublishing.org/doi/10.1098/rspl.1886.0021> [12 February 2020]

25. Lampaert, V., Swevers, J. and Al-Bender, F., 2002. Modification of the Leuven integrated friction model structure. *IEEE Transactions on Automatic Control*, [online] 47(4), pp.683-687. Available at: <https://ieeexplore.ieee.org/stamp/stamp.jsp?tp=&arnumber=995050> [Accessed 5 February 2020].

26. Olssson, H., Astrom, K., deWit, C. and Liscinsky, P., 1995. A New Model for Control of Systems with Friction. *IEEE TRANSACTIONS ON AUTOMATIC CONTROL*, [online] 40, NO. 3, pp.419–425. Available at: <https://ieeexplore.ieee.org/stamp/stamp.jsp?arnumber=376053> [Accessed 5 February 2020].

27. P R Dahl. Solid Friction Model. Technical report, The Aerospace Corporation, El Segundo, Calif., 90245, USA, 1968

28. V. Lampaert, F. Al-Bender and J. Swevers, "A generalized Maxwell-slip friction model appropriate for control purposes," 2003 IEEE International Workshop on Workload Characterization (IEEE Cat. No.03EX775), Saint Petersburg, Russia, 2003, pp. 1170-1177 vol.4.

29. Swevers, J., Al-Bender, F., Ganseman, C. and Projogo, T., 2000. An integrated friction model structure with improved presliding behavior for accurate friction compensation. *IEEE Transactions on Automatic Control*, 45(4), pp.675-686.

30. Olsson, H., Åström, K., Canudas de Wit, C., Gäfvert, M. and Lischinsky, P., 1998. Friction Models and Friction Compensation. *European Journal of Control*, 4(3), pp.176-195.

31. Olfati-Saber, R., 2001. *Nonlinear Control Of Underactuated Mechanical Systems With Application To Robotics And Aerospace Vehicles*. Ph.D. MIT.

32. N/A, 2020. *State Space Representation Of A Mass Spring Damper System | The Robotics Lab*. [online] Roboticslab.ca. Available at: <http://www.roboticslab.ca/mass-spring-damper/> [Accessed 1 March 2020].

33. Yu, H., Liu, Y. and Yang, T. (2008) "Closed-Loop Tracking Control Of A Pendulum-Driven Cart-Pole Underactuated System". *Proceedings Of The Institution Of Mechanical Engineers, Part I: Journal Of Systems And Control Engineering* 222 (2), 109-125

34. Zhang, J., Zhang, Y., Ali, W. and Shieh, L. (2011) *Linearization Modeling For Non-Smooth Dynamical Systems With Approximated Scalar Sign Function* [online] available from

<https://www.researchgate.net/publication/254054675_Linearization_modeling_for_non-smooth_dynamical_systems_with_approximated_scalar_sign_function> [25 February 2020]

35. Li, H., Furuta, K. and Chernousko, F. (2006) "Motion Generation Of The Capsubot Using Internal Force And Static Friction". *Proceedings Of The 45Th IEEE Conference On Decision And Control* 6575–6580

36. Yu, H., Liu, Y. and Yang, T. (2008) "Closed-Loop Tracking Control Of A Pendulum-Driven Cart-Pole Underactuated System". *Proceedings Of The Institution Of Mechanical Engineers, Part I: Journal Of Systems And Control Engineering* 222 (2), 109-125

37. Liu, Y., Yu, H. and Yang, T. (2008) "Analysis And Control Of A Capsubot". *IFAC Proceedings Volumes* 41 (2), 756-761

38. Huda, M., Yu, H. and Wane, S. (2011) "Self-Contained Capsubot Propulsion Mechanism". *International Journal Of Automation And Computing* 8 (3), 348-356

39. Yamagata, Y. and Higuchi, T. (n.d.) "A Micropositioning Device For Precision Automatic Assembly Using Impact Force Of Piezoelectric Elements". *Proceedings Of 1995 IEEE International Conference On Robotics And Automation*

40. Platt, S., Hawks, J. and Rentschler, M. (2009) "Vision And Task Assistance Using Modular Wireless In Vivo Surgical Robots". *IEEE Transactions On Biomedical Engineering* 56 (6), 1700-1710

41. De Falco, I., Tortora, G., Dario, P. and Menciassi, A. (2014) "An Integrated System For Wireless Capsule Endoscopy In A Liquid-Distended Stomach". *IEEE Transactions On Biomedical Engineering* 61 (3), 794-804

42. Yu, H., Nazmul Huda, M. and Samuel Oliver Wane (2011) "A Novel Acceleration Profile For The Motion Control Of Capsubots". *2011 IEEE International Conference On Robotics And Automation*

43. Mahoney, A. and Abbott, J. (2014) "Generating Rotating Magnetic Fields With A Single Permanent Magnet For Propulsion Of Untethered Magnetic Devices In A Lumen". *IEEE Transactions On Robotics* 30 (2), 411-420

44. Rahman, I., Afzal, N. and Patel, P. (2015) "The Role Of Magnetic Assisted Capsule Endoscopy (MACE) To Aid Visualisation In The Upper GI Tract". *Computers In Biology And Medicine* 65, 359-363

45. Simi, M., Valdastri, P., Quaglia, C., Menciassi, A. and Dario, P. (2010) "Design, Fabrication, And Testing Of A Capsule With Hybrid Locomotion For Gastrointestinal Tract Exploration". *IEEE/ASME Transactions On Mechatronics* 15 (2), 170-180

Appendix A – Project Simulation

Simulation

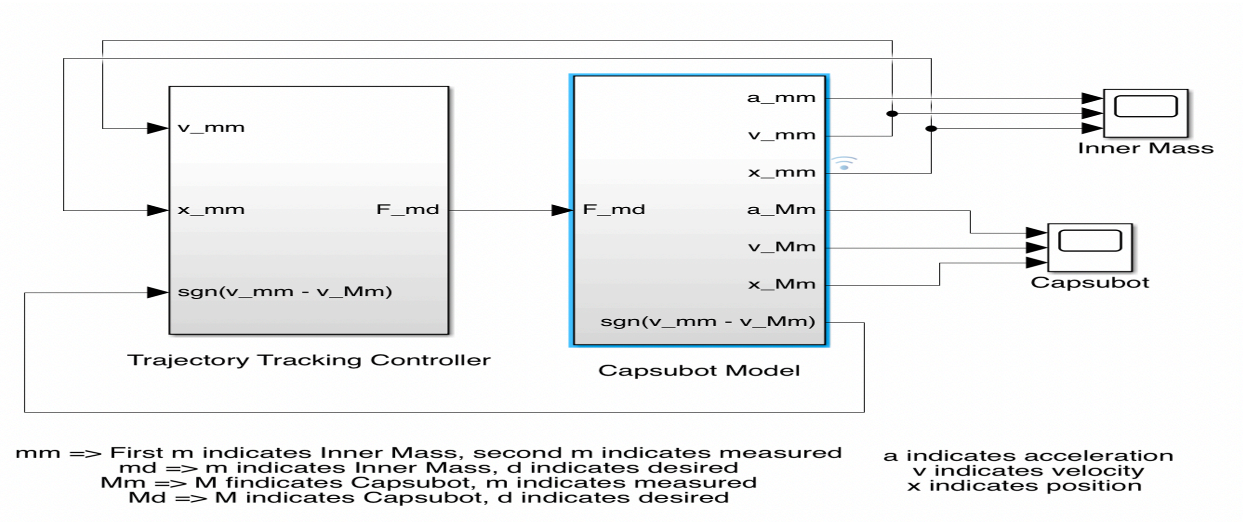

Figure 0.1: Full Simulink model

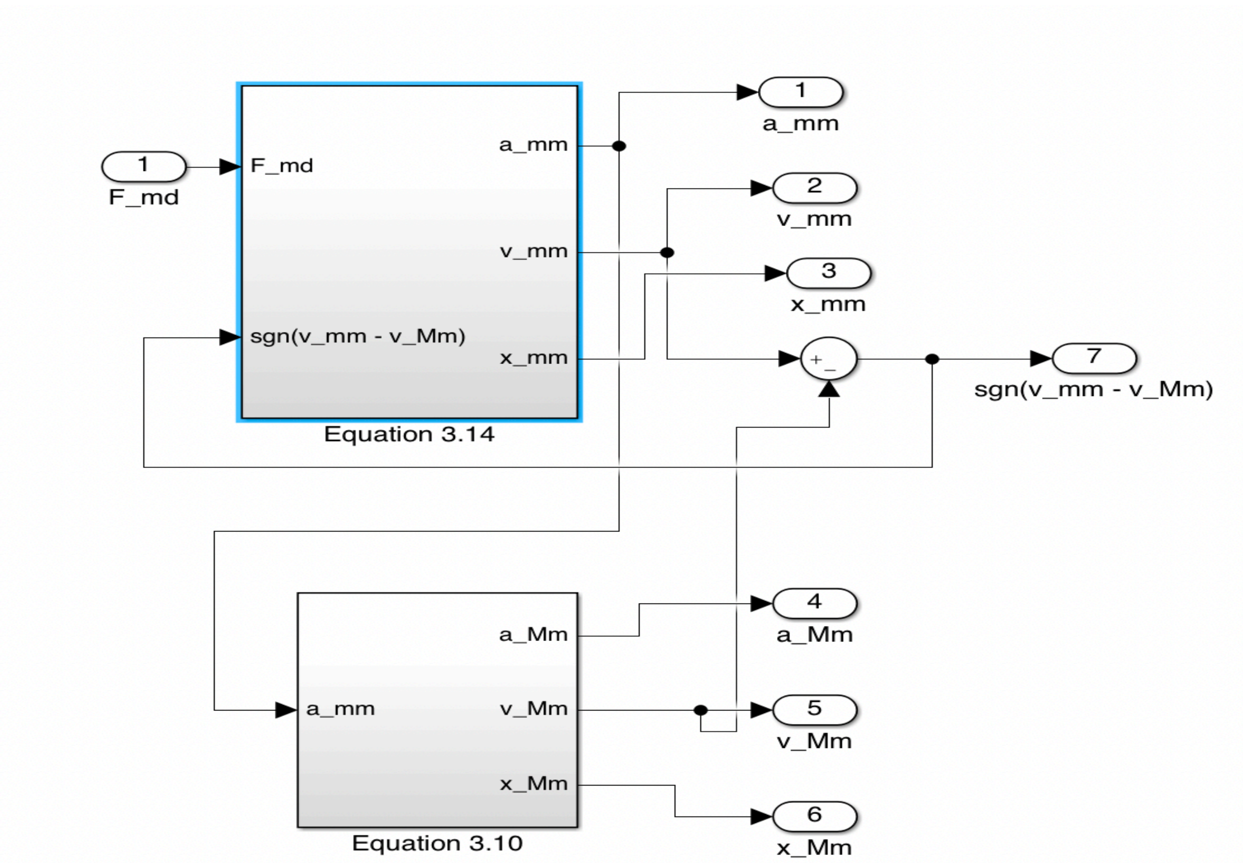

Figure 0.2:Capsubot and Inner mass subsystems

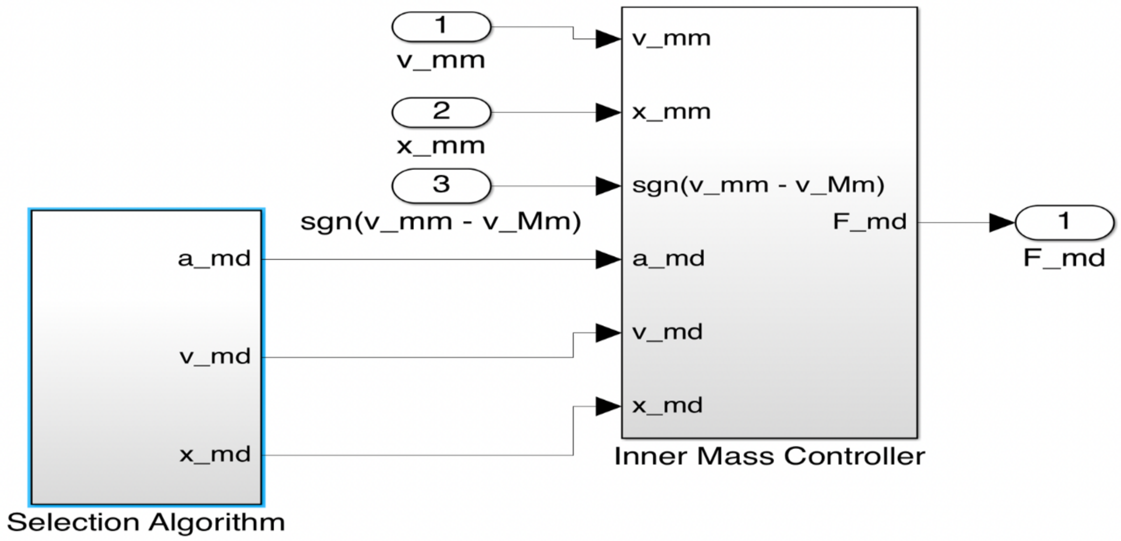

Figure 0.3: inner mass controller and selection algorithms subsystem

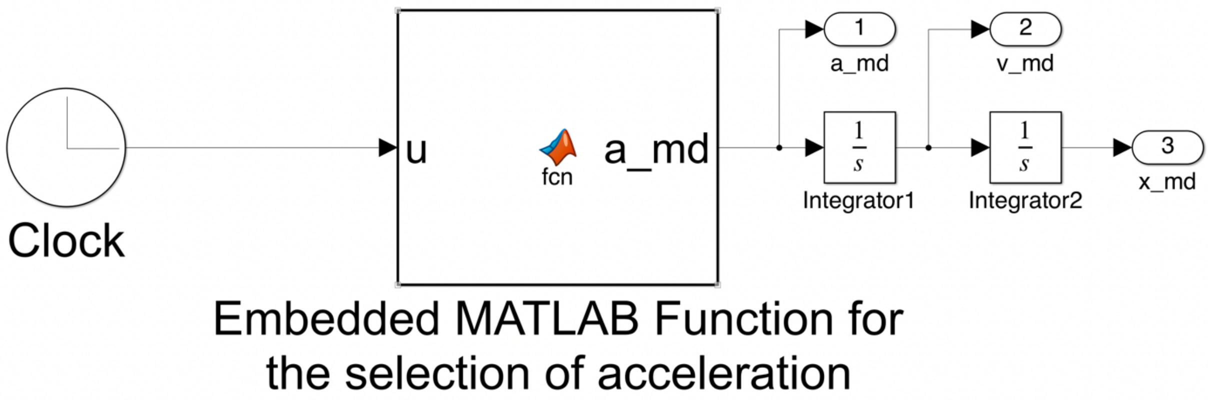

Figure 0.4: selection algorithms model

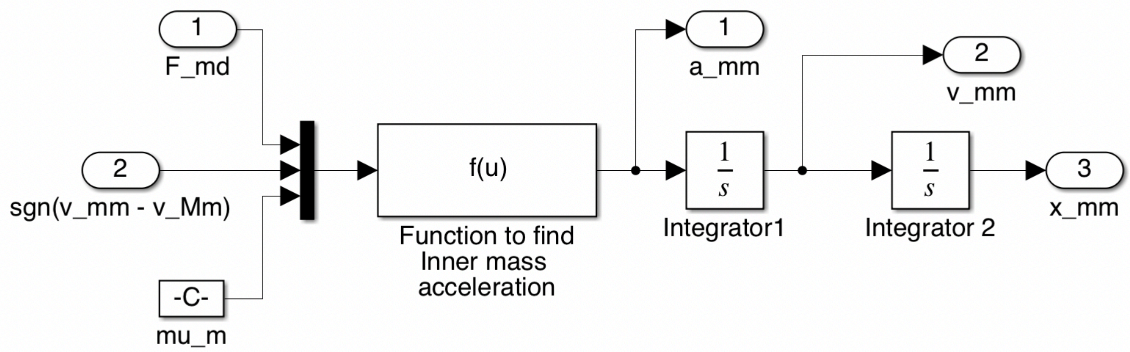

Figure 0.5: Equation (3.1)

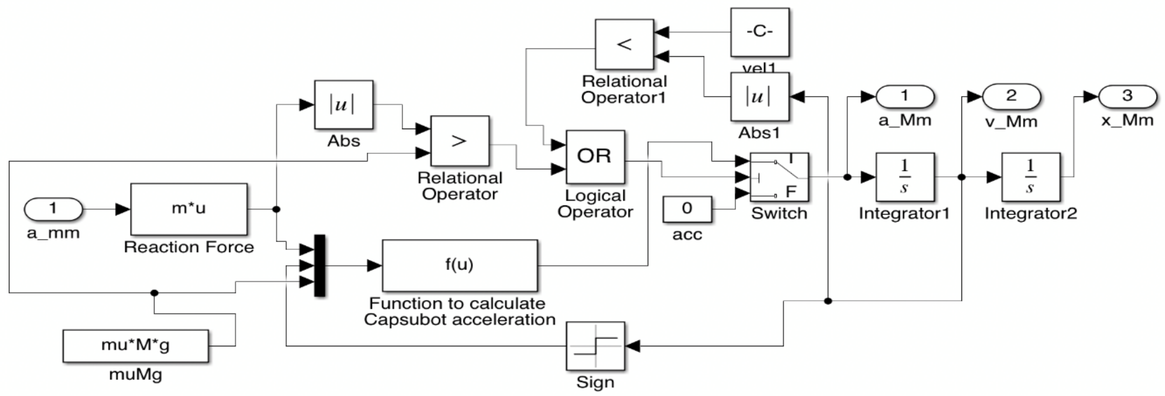

Figure 0.6: Equation (3.2)

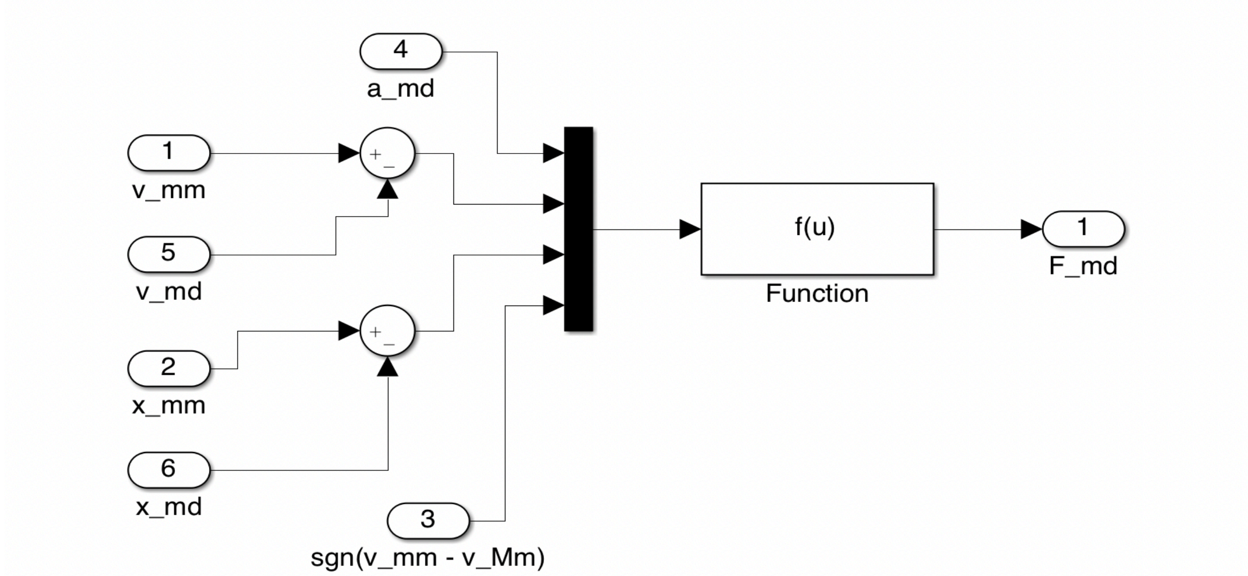

Figure 0.7: Inner mass controller using (4.20) for system with coulombs friction model

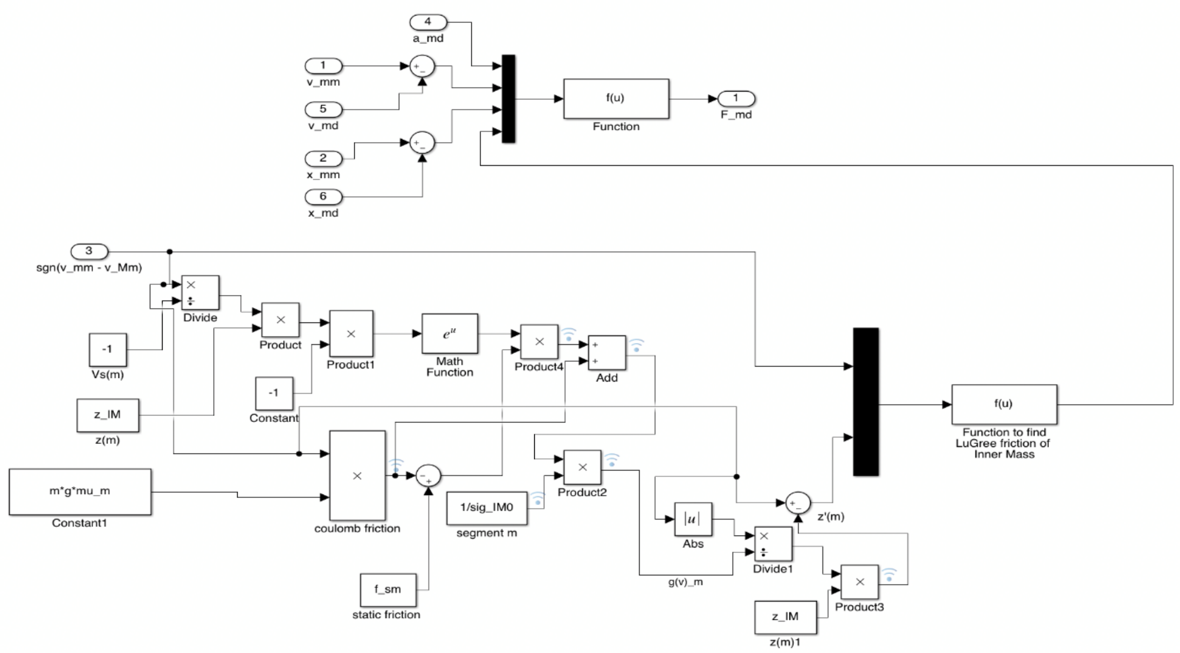

Figure 0.8:Inner mass controller using (4.20) for system with LuGree friction model

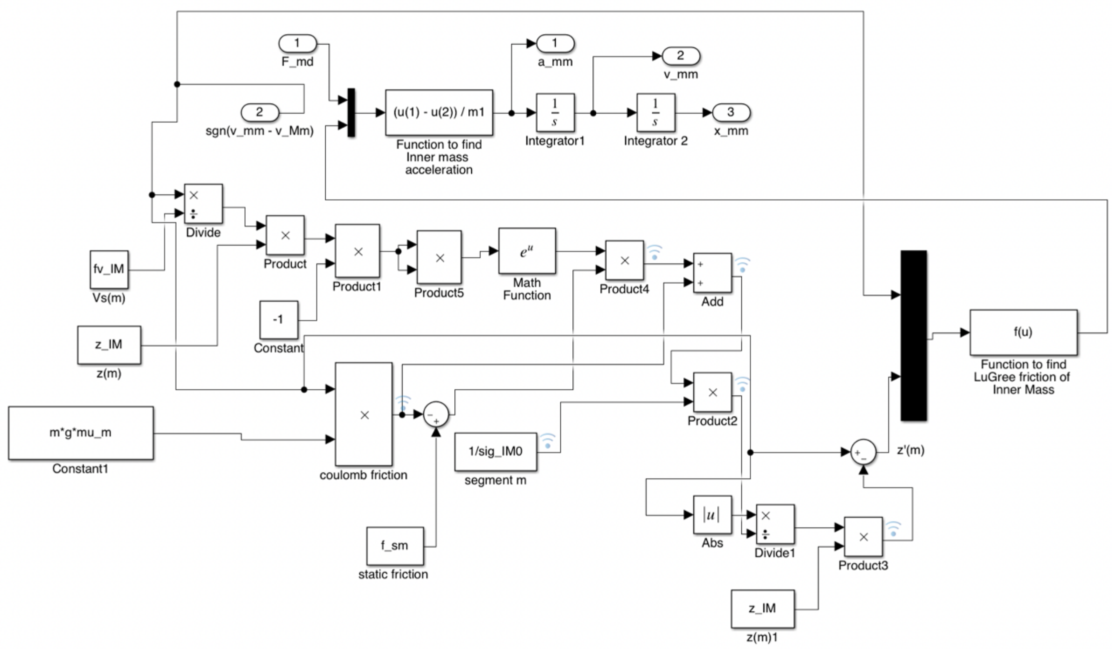

Figure 0.9: Equation (3.14)

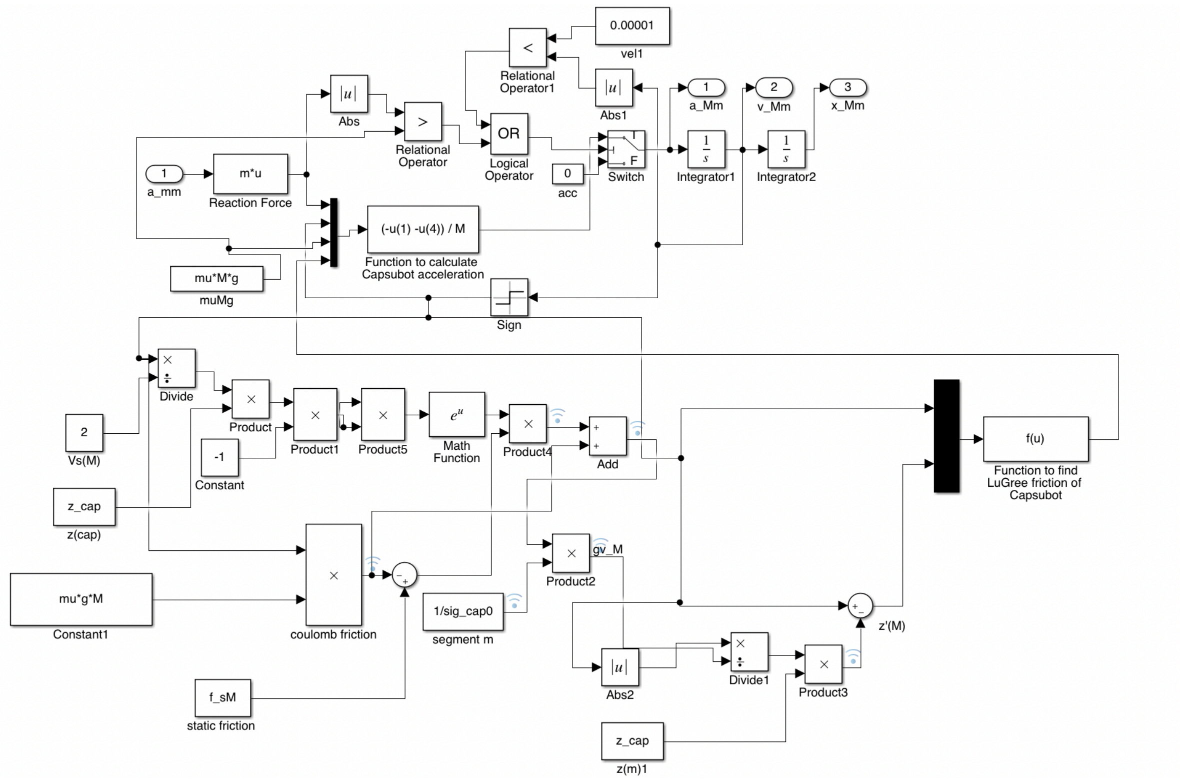

Figure 0.10: Equation (3.10)

Appendix B – log book

Key points and main activities within my logbook

Week 1 (16/September-20/September)

In this week all project ideas was released and I looked into all different projects available and narrowed down the projects to projects within the area of my interest.

Week2. (23/September-27/September)

I contacted supervisors of the projects which I was interested and set up a meeting to discuss the project and get more insight about the projects.

Week3 (30/September- 4/October)

I finalised my decisions and chose path planning and trajectory tracking of miniature 1D capsule robot (capsubot) for medical application project. I had a meeting with my supervisor, on this meeting, an overview of project and how to complete the project brief was given. The main challenges within project was discussed. I started doing background research on underactuated mechanical system dynamic modelling.

Week4 (7/October- 11/October)

On this week I worked on the project brief and also general background research on the project. I also started familiarising myself with programming language required for the project.

Week5 (14/October- 18/October)

On the beginning of this week I had the deadline of the project brief, I submitted the project and also met with my supervisor and a feedback was given regard the project brief. I also started working on my literature review.

Week6 (21/October- 25/October)

On this week I focussed more on my literature review and finding more relevant scientific to my project.

Week7 (28/October- 1/November)

On this week I finished and submitted my literature review, I also met with my supervisor and he gave feedback on literature review, I also spend time working on the capsubot hardware. I also listed additional component required within the hardware.

Week8 (4/November- 8/November)

On this I worked on the ethics approval and also carried on working on the hardware and conducted more research on non-linear control such as lypanov theorem and Jacobean linearization theorem.

Week9 (11/November- 15/November)

I submitted the ethics for the project and component list of the project. Meeting took place within this with supervisor to discuss progress and what needs to be done for the next step.

Week10 (18/November- 22/November)

On this week, I was working on matlab and Simulink to create Simulink models for capsubot and progress report.

Week11 (25/November- 29/November)

On this week I focused more on my progress report and simulation as it was the last week of the preparation stage.

Semester 2

Week 1 (20/Jan-24/Jan)

This was the first week of semester 2 and as my project supervisor left the university and the nature of the project, I did not do much I just focused on doing more research on some background of the project.

Week 2 (27/Jan-31/Jan)

There was not much to do on this week as well as there was no hardware to work, I just carried doing research and simulation.

Week 3 (3/Feb-7/Feb)

On this week, I had a meeting with my new supervisor Dr John, and he informed that the project will be simulation based entirely and we need to develop a new model for the system, he also helped me with some issues I had with simulation.

Week 4(10/Feb-14/Feb)

On this I conducted an intensive background research on different friction models and carried working on the simulation.

Week 5(17/Feb-21/Feb)

On this week I carried on working on the simulation and also finalised my decision to model the system with LuGree friction.

Week 6(24/Feb-28/Feb)

On this week I had meeting with my supervisor, and I presented the idea of modelling the system with the LuGree model and he asked me to develop simulation for it.

Week 7(2/March-6/March)

On this week carried on working on the simulation for the LuGree model.

Week 8(9/March-13/March)

On this week I was working on state representation of both models and writing final report.

Week 9(16/March-20/March)

On this week I had meeting with my supervisor, he asked to do some research on linearization and compare the LuGree model results with coulombs model.

Week 10(23/March-27/March)

On this week more I was working more in coursework’s and partially on my final report.

Week 11(30/March-3/April)

On this week I was doing revision and finishing my coursework’s as well as final report and linearization.

Week 12(6/April-10/April) revision week for exams.

(13/April-21/April) I was working on exams.

(21/April-30/April) on this period I have been working on my final report, presentation and linearization.